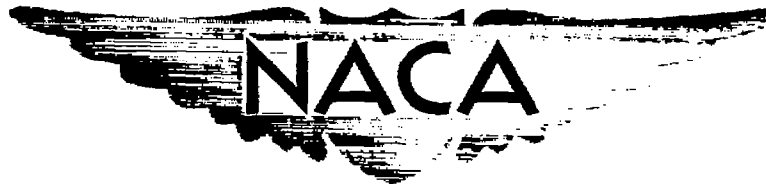


~~CONFIDENTIAL~~

RM A55J12

c. 2

NACA RM A55J12



RESEARCH MEMORANDUM

THE EFFECT OF TRAILING-EDGE BLUNTNESS ON
THE PERFORMANCE OF A SMALL-SCALE
SUPERSONIC PROPELLER AT FORWARD
MACH NUMBERS TO 0.92

By Fred A. Demele and Carl D. Kolbe

Ames Aeronautical Laboratory
Moffett Field, Calif.

UNCLASSIFIED

To

NACA Research

By authority of *Y.R.N. 121* Date *Oct. 14, 1957*

2MT 11-8-57

CLASSIFIED DOCUMENT

This material contains information affecting the National Defense of the United States within the meaning of the espionage laws, Title 18, U.S.C., Secs. 793 and 794, the transmission or revelation of which in any manner to an unauthorized person is prohibited by law.

NATIONAL ADVISORY COMMITTEE
FOR AERONAUTICS

WASHINGTON

January 17, 1956

~~CONFIDENTIAL~~



NATIONAL ADVISORY COMMITTEE FOR AERONAUTICS

RESEARCH MEMORANDUM

THE EFFECT OF TRAILING-EDGE BLUNTNESS ON
THE PERFORMANCE OF A SMALL-SCALE
SUPERSONIC PROPELLER AT FORWARD
MACH NUMBERS TO 0.92

By Fred A. Demele and Carl D. Kolbe


SUMMARY

In order to determine the effects of trailing-edge bluntness on the performance of a supersonic propeller, two three-blade supersonic propellers were tested with blade angles from -19° to 56° throughout a Mach number range extending to 0.92. One propeller, having the designation NACA 1.167-(0)(03)-058, had conventional NACA 16-series sections; the other propeller, designated NACA 1.167-(0)(028)-058, had 16-series sections modified to give trailing-edge bluntness which varied from 100 percent of the maximum section thickness at the blade root to 10 percent of the maximum section thickness at the tip. The blunt-trailing-edge propeller was designed for the same power absorption capabilities and essentially the same torsional stiffness as the sharp-trailing-edge propeller, and hence had slightly thinner blade sections with slightly higher blade stresses. Included in the report are data for the propellers operating in the static- and negative-thrust range.

To investigate the possibility of higher efficiency through the use of airfoils having small leading-edge angles, the sharp-trailing-edge propeller was operated with the blades rotated 180° .

In order to determine the effects of a radially symmetric spinner indentation on propeller performance, a few tests were made with the sharp-trailing-edge propeller in combination with a spinner which was indented by application of Whitcomb's transonic area rule.

The results show that the maximum efficiency of the blunt-trailing-edge propeller was generally from 1 to 3 percent higher than that of the sharp-trailing-edge propeller at Mach numbers of 0.40 and above, and was only slightly lower at Mach numbers below 0.40.

A blacked-out rectangular area at the bottom of the page, likely a redaction of a signature or date.

A comparison of the results obtained in the static- and negative-thrust range indicated that the aerodynamic characteristics of the blunt-trailing-edge propeller were essentially the same as those for the sharp-trailing-edge propeller. The measured static characteristics of the sharp-trailing-edge propeller were compared with calculated values and were found to be in substantial agreement.

INTRODUCTION

It has been generally conceded that the supersonic propeller, in combination with a turbine engine, offers certain advantages as a propulsive device for airplanes flying at high subsonic speeds. In particular, high powers can be absorbed with relatively high efficiency at high subsonic or transonic forward speeds by a propeller of relatively small diameter (ref. 1). However, because of the necessity for thin blades and high rotative speeds, the high disk loading imposes severe structural problems for this type of propeller. It would be desirable if some means were found whereby the steady and vibratory blade stresses could be decreased without a concomitant loss in efficiency or, conversely, whereby the efficiency could be improved for the same blade stresses.

One method which appears attractive in affording this improvement involves the use of blunt trailing edges. A recent investigation at supersonic speeds (ref. 2) has shown that for fairly thick airfoils, increasing the trailing-edge bluntness resulted in only small reductions in maximum lift-drag ratio, whereas the structural section modulus was increased by a large amount. Conversely, for very thin sections, large reductions in maximum lift-drag ratio resulted from increased bluntness, while the section modulus was increased but a slight amount. Thus, for a propeller whose blade elements are operating supersonically it appears that the relatively thick sections near the root should have considerable trailing-edge bluntness, whereas the thin sections near the tip should have nearly sharp trailing edges.

In order to ascertain the effects of trailing-edge bluntness on propeller performance an investigation was undertaken in the 12-foot pressure wind tunnel. The blunt-trailing-edge propeller was designed to have the same power-absorption capabilities and essentially the same blade stresses and flutter characteristics as a sharp-trailing-edge propeller previously tested and reported in reference 3. The experimental data in reference 2 were used as a guide to estimate the characteristics of the blunt-trailing-edge airfoils used in the design of the propeller.

Presented herein are results of force tests of these propellers over a range of blade angles from -19° to 56° and throughout a Mach number range extending up to 0.92. Also included are static- and negative-thrust characteristics of the propellers.

It was conjectured that a propeller having a small leading-edge angle might exhibit higher efficiencies than a propeller having a larger leading-edge angle for conditions wherein the section Mach numbers are greater than unity. To test this hypothesis, the sharp-trailing-edge propeller was operated with the blades rotated 180° .

In order to investigate the possibility of increased propeller performance through spinner indentation, a few additional tests were made with the sharp-trailing-edge propeller in combination with a spinner which was indented by application of Whitcomb's transonic area rule. The indentation was such that the axial distribution of cross-sectional areas of the propeller-spinner combination normal to the thrust axis was essentially the same as that of the original spinner alone.

NOTATION

A	blade section area
A.F.	activity factor, $\frac{100,000}{16} \int_{0.2}^{1.0} \frac{b}{D} \left(\frac{r}{R_t}\right)^3 d\left(\frac{r}{R_t}\right)$
b	blade width
C _p	power coefficient, $\frac{P}{\rho n^3 D^5}$
C _T	thrust coefficient, $\frac{T}{\rho n^2 D^4}$
D	propeller diameter
$\frac{b}{D}$	blade width ratio
E	Young's modulus of elasticity
$(f_\alpha)_c$	calculated blade first-torsion frequency
$(f_\alpha)_M$	measured blade first-torsion frequency
$(f_b)_{\max}$	maximum blade bending stress
$(f_c)_{\max}$	maximum blade centrifugal stress
$(f_h)_M$	measured blade first-bending frequency
$(f_T)_{\max}$	maximum blade total stress

G	shear modulus of elasticity
h	maximum thickness of blade section
$\frac{h}{b}$	blade thickness ratio
(HP) _{full scale}	horsepower, full scale
I_y	section moment of inertia about an axis through the center of gravity, perpendicular to chord line
J	advance ratio, $\frac{V}{nD}$
$(J_T)'_{0.7R_t}$	torsional stiffness constant at 0.7 blade radius, $\left\{ Kbh^3 + \frac{E}{G} \left(\frac{d\beta}{dr} \right)^2 \left[\int (x_b)^4 dA - \frac{I_y^2}{A} \right] \right\}_{0.7R_t}$
K	constant of integration
M	free-stream Mach number
M_t	helical-tip Mach number, $M \sqrt{1 + \left(\frac{\pi}{J} \right)^2}$
n	propeller rotational speed
P	power
r	blade-section radius
R	free-stream Reynolds number per foot
R_t	propeller-tip radius
t	trailing-edge thickness
$\frac{t}{h}$	blade trailing-edge thickness ratio
T	thrust
T.E.	trailing edge
V	free-stream velocity
x_b	chordwise distance to center of twist

β	section blade angle at 0.7 radius
β'	section blade angle
β_F	section blade angle for flexible blade
β_R	section blade angle for rigid blade
η	efficiency, $\frac{C_T}{C_P} J$
η_{\max}	maximum efficiency
ρ	mass density

MODEL AND APPARATUS

The tests were conducted in the Ames 12-foot pressure wind tunnel using the apparatus and test methods described in reference 3. The nacelle assembly was mounted on the tunnel semispan-model force-measuring support system located in the floor of the test section. A schematic drawing of the assembly is shown in figure 1.

Nacelle Assembly

The primary structure of the nacelle assembly consisted of an electric motor and integral gearbox supported by a strut rigidly mounted to the framework of the six-component balance system. The secondary structure, which was rigidly attached to the tunnel floor, consisted of a fairing enclosing the afterportion of the motor and support strut. A clearance gap and concentric rubber seal were provided between the primary and secondary structure as shown in figure 1. A more detailed description of the nacelle assembly can be found in reference 3.

Power Transmission Unit

Power was supplied to the propeller through the gearbox by an electric motor having a rating of 66 horsepower at 18,000 revolutions per minute. Continuous speed control was accomplished by means of a variable-frequency power supply. Motor speed indication was provided by a frequency-measuring instrument connected to a variable-reluctance alternator on the rear of the motor.

Spinners

The major portion of the investigation was made using a spinner having an NACA 1-series profile. A few tests were made of the sharp-trailing-edge propeller in combination with a spinner whose NACA 1-series profile was indented in the region of the blades to minimize adverse effects of compressibility. The modification was made in accordance with Whitcomb's transonic area rule (ref. 4). For the sake of simplicity, the propeller-spinner combination was considered to be analogous to a wing-body combination in an airstream parallel to the longitudinal body axis. The spinner indentation was such that the cross-sectional areas normal to the thrust axis for the propeller-spinner combination ($\beta = 51^\circ$) were essentially the same as for the original NACA 1-series spinner alone. Coordinates of both spinners are given in table I.

A clearance gap (0.015 inch) was provided between the spinners and the forward face of the power transmission unit. Individual spinners were provided with blade cutouts corresponding to each blade angle. The gap between the propeller blades and the spinner was unsealed for the major portion of the investigation.

Propellers

The supersonic propellers used in this investigation were 1/12-scale and had the same full-scale design condition. This condition was stipulated as an advance ratio of 2.01 at a forward Mach number of 0.83 and an altitude of 40,000 feet. The design power was approximately 3500 horsepower with a propeller efficiency of 70 percent; the corresponding design blade angle at 0.70 radius was approximately 46° . It should be noted that the power was previously reported (ref. 3) to be 5000 horsepower with a propeller efficiency of 75 percent. The latter values were based on strip-theory calculations which neglected the induction effects, since at that time it was felt that these effects were very small for a supersonic propeller operating at high subsonic forward Mach numbers. However, the concept of negligible induction effects for compressible flow has since been discarded (e.g., see ref. 5). The performance calculations made for the design condition and reported herein have included the effects of propeller induction (ref. 6).

The NACA 1.167-(0)(03)-058 three-blade propeller had a diameter of 14 inches and had NACA 16-series blade sections. With the exception of a slight decrease in blade thickness ratios, the NACA 1.167-(0)(028)-058 propeller differed from its predecessor only in that the blade sections were of the NACA 16-series modified to have trailing edges of finite thickness which were faired into the original contour by straight tangent lines. The modification incorporated trailing-edge bluntness which varied

from 100 percent of the maximum section thickness at the blade root to 10 percent of the maximum section thickness at the tip (fig. 2). The design of the blunt-trailing-edge propeller was predicated on the concept of maintaining the same power absorption capabilities and torsional rigidity as the NACA 1.167-(0)(03)-058 propeller. In addition, it was felt desirable to maintain essentially the same level of blade stress. The degree to which these design criteria have been compromised is indicated in the following table:

Design characteristics of the blunt- and the sharp-trailing-edge propellers		
Characteristic	NACA 1.167-(0)(03)-058	NACA 1.167-(0)(028)-058
Blade section	16-00x	Modified 16-00x having blunt T.E.
A.F.	188.4	188.4
β_R	46.34°	46.00°
β_F	47.49°	47.49°
(HP) full scale	3500	3600
η	70 percent	71 percent
$(J_T)'_{0.7R}$	1.3×10^{-4}	1.3×10^{-4}
$(f_a)_c$	1067 cps	1072 cps
$(f_a)_M$	1098 cps	1064 cps
$(f_h)_M$	169.8 cps	139.1 cps
$(f_b)_{max}$	12,200 psi, $r/R_t = 0.64$	15,000 psi, $r/R_t = 0.58$
$(f_c)_{max}$	33,000 psi, $r/R_t = 0.60$	34,500 psi, $r/R_t = 0.54$
$(f_T)_{max}$	45,000 psi, $r/R_t = 0.60$	49,200 psi, $r/R_t = 0.57$

The torsional frequency was held nearly equal for the two designs in an effort to provide both propellers with the same stall-flutter boundaries. Both the bending stresses and the centrifugal stresses were slightly higher for the blunt propeller, and this increase in blade stress should be considered when comparing the relative merits of the two propellers.

Both propellers were constructed of heat-treated alloy steel. Blade-form curves are presented in figure 2 and a photograph of the blades is shown in figure 3.

TEST CONDITIONS

Measurements of thrust, power, and rotational speed were made for both the NACA 1.167-(0)(03)-058 (sharp-trailing-edge) propeller and the NACA 1.167-(0)(028)-058 (blunt-trailing-edge) propeller at various blade angles, Mach numbers, and Reynolds numbers. The configurations and range of conditions investigated are given in table II.

The procedure for obtaining data involved operation of each propeller at a predetermined Mach number and Reynolds number throughout a range of rotational speeds. Operation of each propeller was limited by one or more of the following factors:

1. Maximum rotational speed of propeller shaft (27,000 rpm).
2. Maximum power output of motor (66 hp).
3. Thrust (positive or negative) at which estimated blade stresses were 100,000 lb/sq in.
4. Auricular evidence of stall flutter.

REDUCTION OF DATA

Propeller Thrust

As used herein, propeller thrust is the difference between the longitudinal force produced by the propeller operating in combination with the spinner and nacelle forebody¹ and the longitudinal force on the spinner and nacelle forebody in the absence of the propeller at the same Mach number and Reynolds number. The longitudinal force was measured by the six-component balance system.

Propeller Power

In order to determine the power absorbed by the propeller, the motor and gearbox were calibrated in the absence of the propeller throughout the range of rotational speeds and torques utilized during the investigation. No torque correction was applied for spinner skin friction since it was a negligible part of the combined power loss.

¹The nacelle forebody is that portion of the nacelle between the rear face of the spinner and the clearance gap (see fig. 1).

Corrections

The data have been corrected for the effect of tunnel-wall constraint on the velocity in the region of the propeller plane by the method of reference 7. The magnitude of the maximum correction applied to the data was 0.7 percent. The constriction effects due to operating the propellers were evaluated by the method of references 8 and 9 and were found to be negligible.

The data were also corrected to take account of the pressure difference acting across the concentric seal (fig. 1). The force resulting from this pressure difference was applied to the measured longitudinal force.

Accuracy of Data

Analysis of the sources of error and correlation of test data for duplicate conditions indicated the maximum probable errors in the data were as follows:

M	β , deg	J	C_T	C_P	η
0 to 0.082	± 0.15	± 0.01	± 0.005	± 0.006	- - -
0.24 to 0.92	$\pm .15$	$\pm .01$	$\pm .002$	$\pm .002$	± 0.015

In the negative-thrust range, where the advance ratio was large, the error in thrust and power coefficients may have been considerably greater than shown in the foregoing table.

RESULTS

The results of this investigation are presented in figures 4 through 21. Table II is an index of these figures and indicates the coefficients and range of variables given in each figure. Presented in figure 4 is a comparison of characteristics of the propeller-spinner-nacelle combination with previously unreported results of tests of the propeller-spinner combination which was described in reference 10. Presented in figures 5 through 11 are the basic propeller characteristics for various Mach numbers and Reynolds numbers. The effects of Mach number and advance ratio

on maximum efficiency are shown in figures 12 through 14. The propeller characteristics in the negative-thrust range are presented in figures 15 through 18, and the static characteristics are presented in figures 19 through 21.

It should be noted that in figures containing data for both propellers, the identifying blade angle refers to the sharp-trailing-edge propeller. For these cases the blade angles for the blunt-trailing-edge propeller were 0.5° larger than the corresponding blade angles for the sharp-trailing-edge propeller.

It will be noted that the data from this investigation have been supplemented with data reported in reference 3, thereby affording a more comprehensive presentation. A comparison of the characteristics of the NACA 1.167-(0)(03)-058 propeller from reference 3 with those from this investigation indicated the differences were of the order of the accuracy of the data stated earlier in this report.

DISCUSSION

It should be mentioned that the efficiencies presented herein have been somewhat penalized by the inclusion, in the measured thrust, of the nacelle drag due to the propeller slipstream. This can readily be seen in figure 4 wherein the characteristics of the propeller-spinner-nacelle combination are compared with the characteristics of the propeller-spinner combination which was described in reference 10. Although the comparison was limited to a blade angle of 56° , the data indicate that the maximum efficiencies presented in this report are about 2 percent lower at a Mach number of 0.80 and about 6 percent lower at a Mach number of 0.90 than the maximum efficiencies of the isolated propeller-spinner combination.

Design-Performance Comparisons

The degree to which the measured propeller characteristics agree with the calculated characteristics at the design condition for the full-scale propellers ($M = 0.83$; $D = 14$ ft; altitude = 40,000 ft) may be seen in the following table. The calculated values of power and efficiency were obtained by strip theory employing Theodorsen's circulation functions from reference 6.

Characteristic	Blunt trailing edge		Sharp trailing edge	
	Calculated	Measured	Calculated	Measured
HP	3600	3600	3500	3500
η , percent	71	76	70	73
J	2.01	2.01	2.01	2.01
β , deg	46.0	45.6	46.3	46.0

It may be noted that for both the blunt- and sharp-trailing-edge propellers the design horsepower was attained at approximately the design blade angle, but that the efficiency was higher than calculated. The measured efficiency was higher for the blunt- than for the sharp-trailing-edge propeller, that is, 76 percent compared to 73 percent. It should be noted that the higher efficiency achieved with the blunt-trailing-edge propeller is a result of both trailing-edge bluntness and decreased blade thickness. The agreement between the measured and calculated efficiency was less satisfactory for the blunt-trailing-edge propeller, and it is felt that lack of sufficient two-dimensional data for blunt-trailing-edge airfoils is responsible for most of this disagreement.

Effects of Mach Number

The maximum efficiency in figure 5 is shown as a function of forward Mach number in figure 12. For the blunt-trailing-edge propeller, the maximum efficiency varied from about 83 percent at a Mach number of 0.60 to about 65 percent at a Mach number of 0.92. For blade angles of 41° and above, the maximum efficiency of the blunt-trailing-edge propeller was generally from 1 to 3 percent higher than for the sharp-trailing-edge propeller. It is considered noteworthy that at a Mach number of 0.24 the efficiency of the blunt-trailing-edge propeller was only 1 or 2 percent less than that of the sharp-trailing-edge propeller. For these conditions the Mach numbers near the blade-spinner juncture were less than 0.5, and therefore one might have anticipated a larger loss in efficiency due to the high drag of two-dimensional blunt-trailing-edge airfoils in this speed regime.

The variation of maximum efficiency with tip Mach number for both propellers is shown in figure 13. In the range of blade angles from 31° to 41° , the maximum efficiency generally increased slightly up to a tip Mach number of about 1.1 and then decreased beyond this point. This decrease with increasing tip Mach number is indicated for blade angles of 36° and above, the rate of change of maximum efficiency with tip Mach number becoming more rapid with increasing blade angle.

The variation of maximum efficiency with advance ratio for both propellers at Mach numbers from 0.24 to 0.92 may be seen in figure 14. At

a forward Mach number of 0.24 the maximum efficiency increased up to an advance ratio of about 1.2 and thereafter remained fairly constant for a given Mach number. However, there is a slight indication of increased efficiency as the advance ratio decreases toward the design value of 2.01 for Mach numbers of 0.83 and above. The higher maximum efficiency of the blunt-trailing-edge propeller (from 1 to 3 percent) is again evidenced by these curves in the range of Mach numbers from 0.60 to 0.92.

Effects of Reynolds Number

The improvement in the aerodynamic characteristics of the blunt-trailing-edge propeller due to changing the Reynolds number from 800,000 to 1,600,000 is indicated in figure 7. An increase in maximum efficiency of about 5 percent resulted at a Mach number of 0.60, whereas at a Mach number of 0.90 the improvement was about 2 percent. Increasing the Reynolds number from 800,000 to 1,600,000 also improved the maximum efficiency of the sharp-trailing-edge propeller, although the increase was usually 3 percent or less, as shown in figure 8.

Effect of Sealed Blade-Spinner Juncture

In order to prevent air spillage around the blade root, the gap between the blade and spinner was sealed for a few tests. The data in figure 9 indicate the improvement afforded by this procedure averaged approximately 3 percent at Mach numbers of 0.83 and below, but there was no increase in efficiency at higher Mach numbers.

Effect of Spinner Indentation

The effect of a radially symmetric indentation of the spinner in the region of the propeller blades on the characteristics of the sharp-trailing-edge propeller may be seen in figure 10. It is evident that no improvement was afforded in the range of Mach numbers from 0.70 to 0.86, but the data indicate a 3-percent increase in maximum efficiency at Mach numbers of 0.90 and 0.92. Actually, efficiency increases were expected even at a Mach number of 0.83, since the blade-section Mach numbers in the region of the spinner juncture were near unity for this condition. The lack of more significant improvement might be attributed to the increased blade area exposed by the spinner indentation. The blade thickness increased rather abruptly in this region, and the resultant drag rise probably canceled any improvement due to indentation.

Due to the limited nature of this particular investigation, the data in figure 10 are somewhat inconclusive and more extensive tests of indented spinners should be undertaken to determine their effects on propeller performance.

Effect of Reversed Blade Section

The NACA 1.167-(0)(03)-058 propeller was also operated with the sharp trailing edge facing forward, that is, with the blade rotated 180° . It was conjectured that the section pressure drag would be reduced because of the smaller leading-edge angle, and that this reduction might be reflected in higher efficiencies for conditions wherein the section Mach numbers were greater than unity. The results of these tests as shown in figure 11 indicate slightly lower maximum efficiencies for the reversed-blade propeller in the range of Mach numbers from 0.60 to 0.80. Above this range of Mach numbers the level of efficiency was approximately the same for both propellers, although the data indicate possible slight efficiency increases due to reversing the blade sections at Mach numbers of 0.90 and 0.92.

Negative-Thrust Characteristics

The basic characteristics of both propellers in primarily the negative-thrust range are shown in figure 15 for a Mach number range of 0.24 to 0.92 and in figures 16 and 17 for a Mach number of 0.082. The data in the latter figures have been plotted as a function of blade angle in figure 18 for two representative values of advance ratio. The negative-thrust characteristics of the blunt-trailing-edge propeller were essentially the same as those for the sharp-trailing-edge propeller throughout the entire range of Mach numbers.

Static Characteristics

The static characteristics of the blunt- and sharp-trailing-edge propellers are presented in figures 19 and 20, respectively, as functions of the product of the rotational speed and the diameter. Included in figure 20 is a comparison with values calculated by the strip-theory method of reference 11. The agreement between the measured and calculated characteristics is considered to be good for the blade angles ($\beta = 6^\circ, 16^\circ$) investigated. The lack of more extensive data for NACA 16-series airfoils prevented reliable calculations for blade angles higher than 16° , and it was even necessary to extrapolate the data to obtain the blade loading for stations inboard of 0.5 radius at a blade angle of 16° .

The data in figures 19 and 20 have been summarized in figure 21, wherein the thrust and power coefficients and the ratio of thrust coefficient to power coefficient have been presented as functions of blade angle. The curves of the ratio of thrust coefficient to power coefficient have been deleted near zero blade angle because of the percentage inaccuracy of the power data near zero power.

CONCLUDING REMARKS

An investigation was conducted on two three-blade supersonic propellers, the NACA 1.167-(0)(03)-058 (sharp trailing edge) and the NACA 1.167-(0)(028)-058 (blunt trailing edge), for blade angles ranging from -19° to 56° throughout a Mach number range extending up to 0.92. The blunt-trailing-edge propeller was designed to have the same power absorption capabilities and essentially the same torsional stiffness as the sharp-trailing-edge propeller, but with slightly higher blade stresses. The results show the following:

1. At Mach numbers of 0.40 and above, the maximum efficiency of the blunt-trailing-edge propeller was generally from 1 to 3 percent higher than that of the sharp-trailing-edge propeller, and was only slightly lower below a Mach number of 0.40.

2. The static- and negative-thrust characteristics of the blunt-trailing-edge propeller were similar to those of the sharp-trailing-edge propeller.

3. The agreement between the measured and calculated static characteristics for blade angles up to 16° was good.

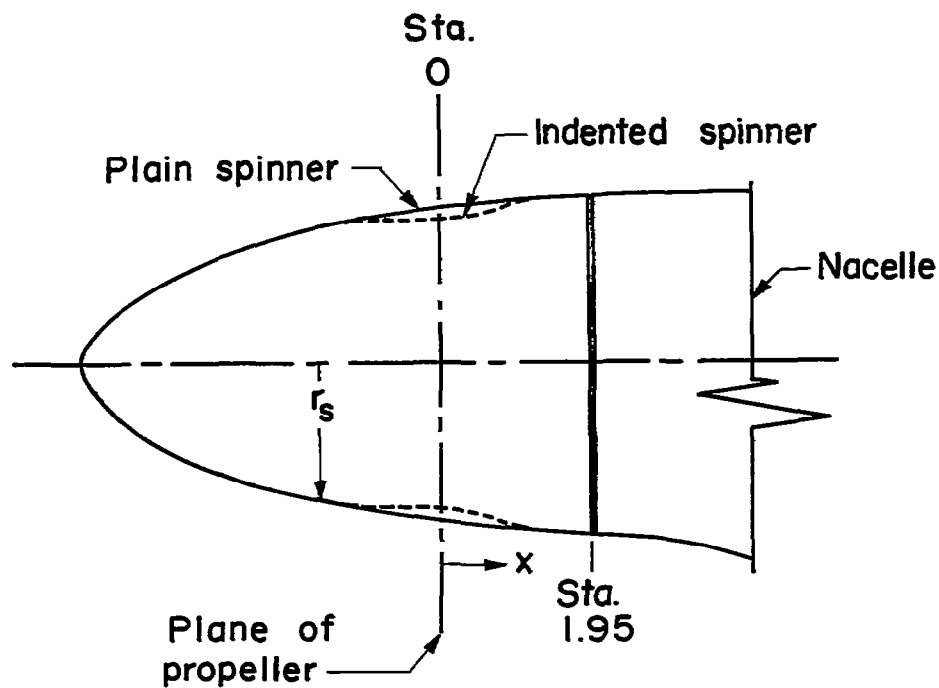
Ames Aeronautical Laboratory
National Advisory Committee for Aeronautics
Moffett Field, Calif., Oct. 12, 1955

REFERENCES

1. Evans, Albert J., and Liner, George: A Wind-Tunnel Investigation of the Aerodynamic Characteristics of a Full-Scale Supersonic-Type Three-Blade Propeller at Mach Numbers to 0.96. NACA RM L53F01, 1953.
2. Katzen, Elliot D., Kuehn, Donald M., and Hill, William A.: Investigation of the Effects of Profile Shape on the Aerodynamic and Structural Characteristics of Thin, Two-Dimensional Airfoils at Supersonic Speeds. NACA RM A54B08a, 1954.
3. Demele, Fred A., and Otey, William R.: Investigation of the NACA 1.167-(0)(03)-058 and NACA 1.167-(0)(05)-058 Three-Blade Propellers at Forward Mach Numbers to 0.92 Including Effects of Thrust-Axis Inclination. NACA RM A53F16, 1953.
4. Whitcomb, Richard T.: A Study of the Zero-Lift Drag-Rise Characteristics of Wing-Body Combinations Near the Speed of Sound. NACA RM L52H08, 1952.
5. Davidson, Robert E.: Linearized Potential Theory of Propeller Induction in a Compressible Flow. NACA TN 2983, 1953.
6. Glover, L. S., and Borst, H. V., comps.: Application of Theodorsen's Theory to Strip Analysis Procedure For Single Rotation Propellers. Rep. No. C-2070, Curtiss-Wright Corp., Propeller Division, Caldwell, N. J., Sept. 2, 1949.
7. Herriot, John G.: Blockage Corrections for Three-Dimensional-Flow Closed-Throat Wind Tunnels, With Consideration of the Effect of Compressibility. NACA Rep. 995, 1950. (Formerly NACA RM A7B28)
8. Glauert, H.: The Elements of Airfoil and Airscrew Theory. The Univ. Press, Cambridge, Eng. Also available from Macmillan Co., N.Y., 1943, pp. 222-226.
9. Young, A. D.: Note on the Application of the Linear Perturbation Theory to Determine the Effect of Compressibility on the Wind Tunnel Constraint on a Propeller. R.&M. No. 2113 (8301) British A.R.C., Nov. 1944. Also issued as British R.A.E. TN No. Aero. 1539, Nov. 1944.
10. Demele, Fred A., and Otey, William R.: Investigation of the Normal Force Accompanying Thrust-Axis Inclination of the NACA 1.167-(0)(03)-058 and the NACA 1.167-(0)(05)-058 Three-Blade Propellers at Forward Mach Numbers to 0.90. NACA RM A54D22, 1954.

11. Swihart, John M.: Experimental and Calculated Static Characteristics of a Two-Blade NACA 10-(3)(063)-045 Propeller. NACA RM L54A19, 1954.

TABLE I.- COORDINATES OF PROPELLER SPINNERS



Distance from station 0 x	Radius, r_s	
	Plain	Indented
-5.00	0	0
-4.79	.385	.385
-4.58	.567	.567
-4.25	.788	.788
-3.95	.951	.951
-3.25	1.242	1.242
-2.55	1.472	1.472
-2.41	1.512	1.512
-1.85	1.658	1.658
-1.20	1.800	1.800
-1.00	1.836	1.820
-.80	1.871	1.836
-.40	1.933	1.832
0	1.985	1.845
.40	2.027	1.946
1.08	2.077	2.077
1.95	2.100	2.100

All dimensions are in inches;
sketch not to scale.

TABLE II.- INDEX OF DATA FIGURES

Fig. No.	Plot	Mach number, M	Reynolds No. per ft, $R \times 10^{-6}$	Blade angle, β , deg	Configuration
4	C_T, C_p, η , vs. J	0.80 to 0.90	1.6	56	Propeller-spinner and propeller-spinner nacelle
5	C_T, C_p, η, M_t , vs. J	0.24 to 0.92	1.6	21 to 56	sharp T.E. and blunt T.E.
6	C_T, C_p , vs. J	0.082	1.15	16 to 36	sharp T.E. and blunt T.E.
7	C_T, C_p, η , vs. J	0.60 to 0.90	0.8, 1.6	46, 51	blunt T.E.
8		0.70 to 0.90	0.8, 1.6	51	sharp T.E.
9		0.70 to 0.92	1.6	51	sealed and unsealed gap
10		0.70 to 0.92	1.6	51	plain and indented spinner
11		0.60 to 0.92	1.6	46	normal and reversed blade section
12	η_{max} vs. M	0.24 to 0.92	1.6	21 to 56	sharp T.E. and blunt T.E.
13	η_{max} vs. M_t	0.24 to 0.92	1.6	21 to 56	sharp T.E. and blunt T.E.
14	η_{max} vs. J	0.24 to 0.92	1.6	21 to 56	sharp T.E. and blunt T.E.
15	C_T, C_p vs. J (neg range)	0.24 to 0.92	1.6	21 to 56	sharp T.E. and blunt T.E.
16	C_T, C_p vs. J (neg range)	0.082	1.15	-19 to 36	blunt T.E.
17	C_T, C_p vs. J (neg range)	.082	1.15	-19 to 36	sharp T.E.
18	C_T, C_p vs. β (neg range)	.082	1.15	-19 to 36	sharp T.E. and blunt T.E.
19	C_T, C_p vs. nD	0	0	-19 to 36	blunt T.E.
20	C_T, C_p vs. nD	0	0	-19 to 56	sharp T.E.
21	$C_T, C_p, C_T/C_p$ vs. β	0	0	-19 to 56	sharp T.E. and blunt T.E.

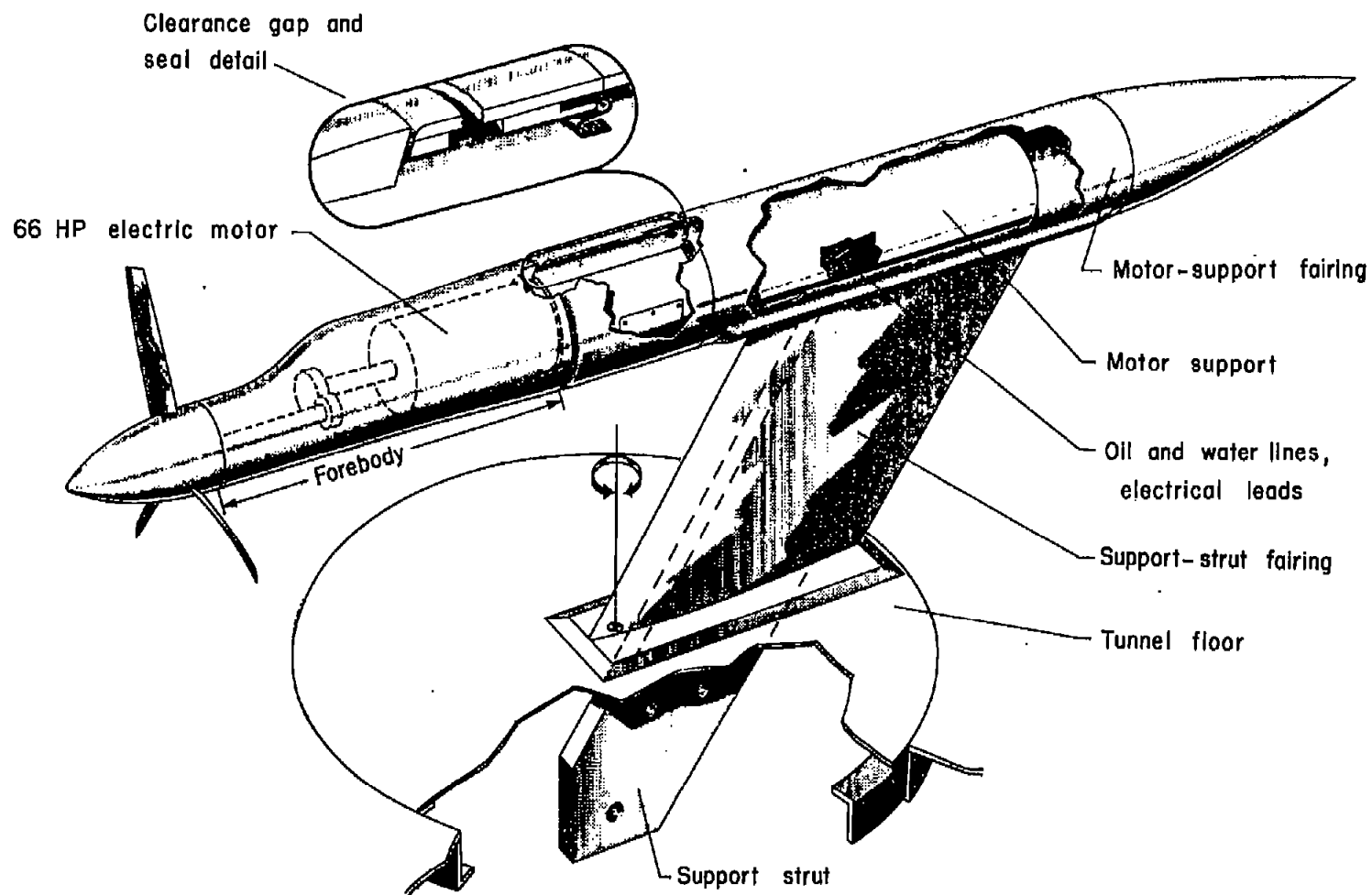


Figure 1.- Nacelle assembly.

Developed plan form

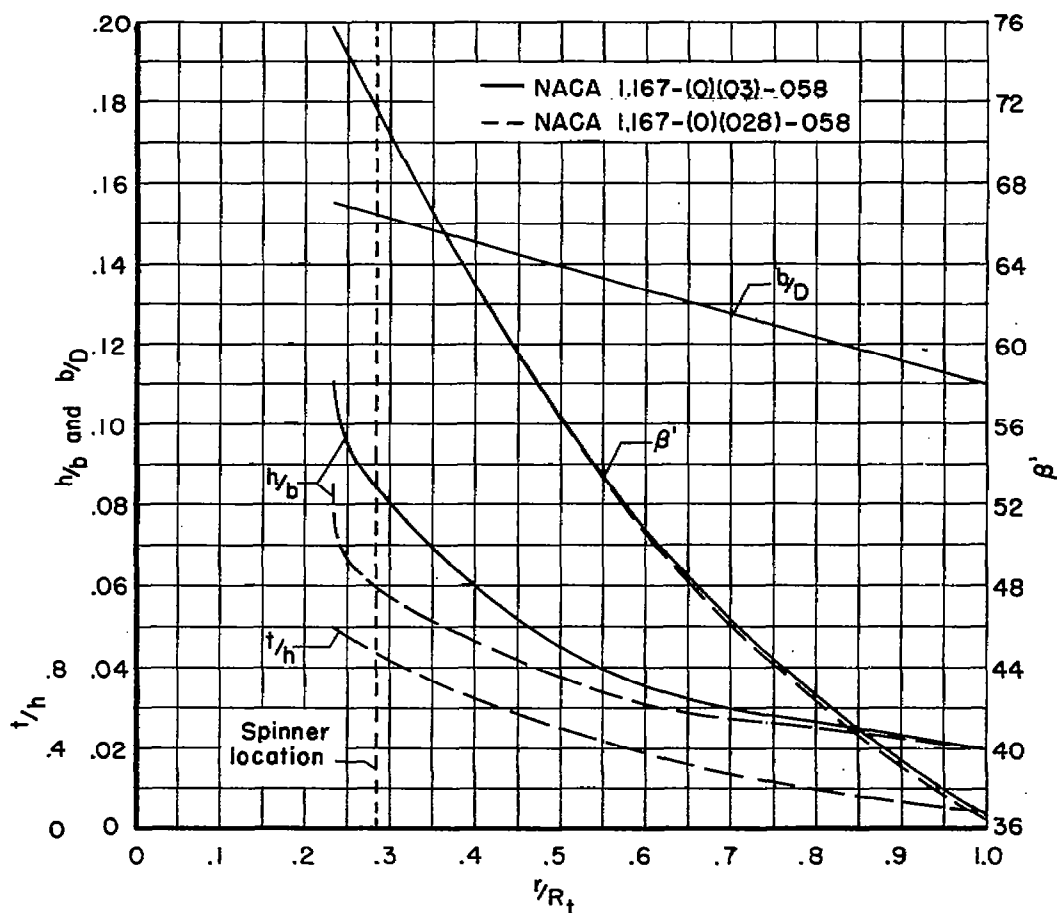
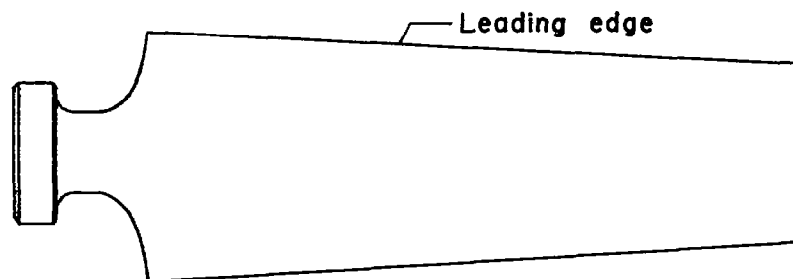
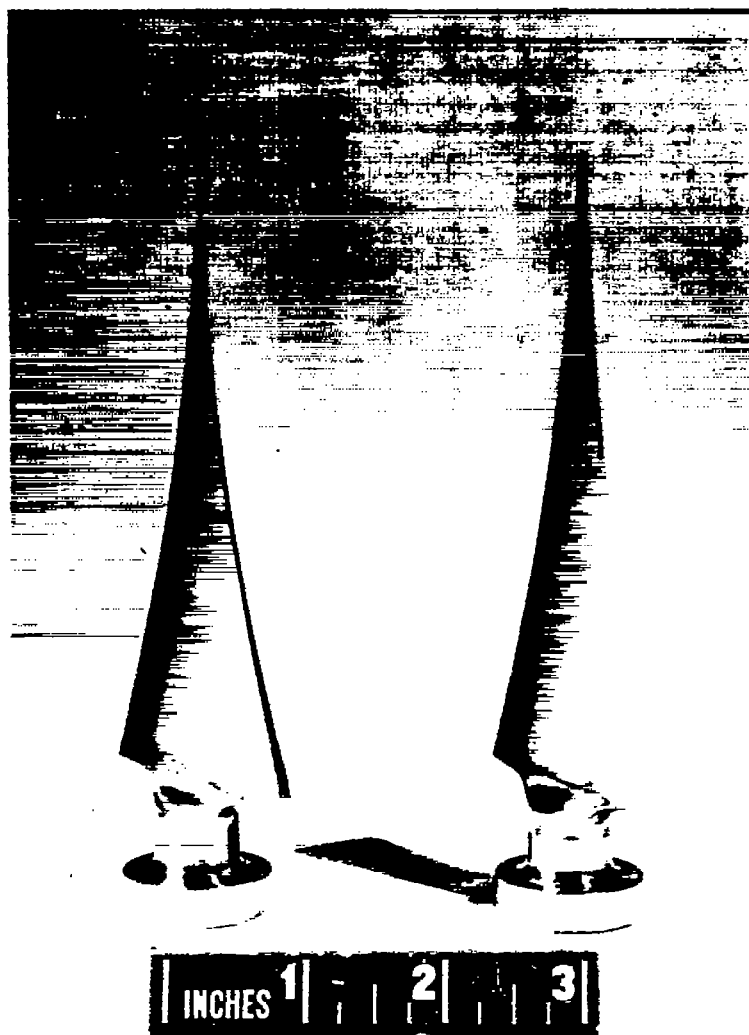


Figure 2.- Blade-form curves for the NACA 1.167-(0)(03)-058, sharp-trailing-edge, and the NACA 1.167-(0)(028)-058, blunt-trailing-edge, three-blade propellers.



$$\frac{b}{D} = .12$$

$$b = .12 \times 14$$

$$\frac{1.68}{1.2} = 1.4$$

$$1.4 \times 0.14 = 0.196$$

$$\frac{.14}{.00000} = 12.22222$$

A-19614

Figure 3.- Photograph of the NACA 1.167-(0)(028)-058, blunt-trailing-edge, and the NACA 1.167-(0)(03)-058, sharp-trailing-edge propeller blades.

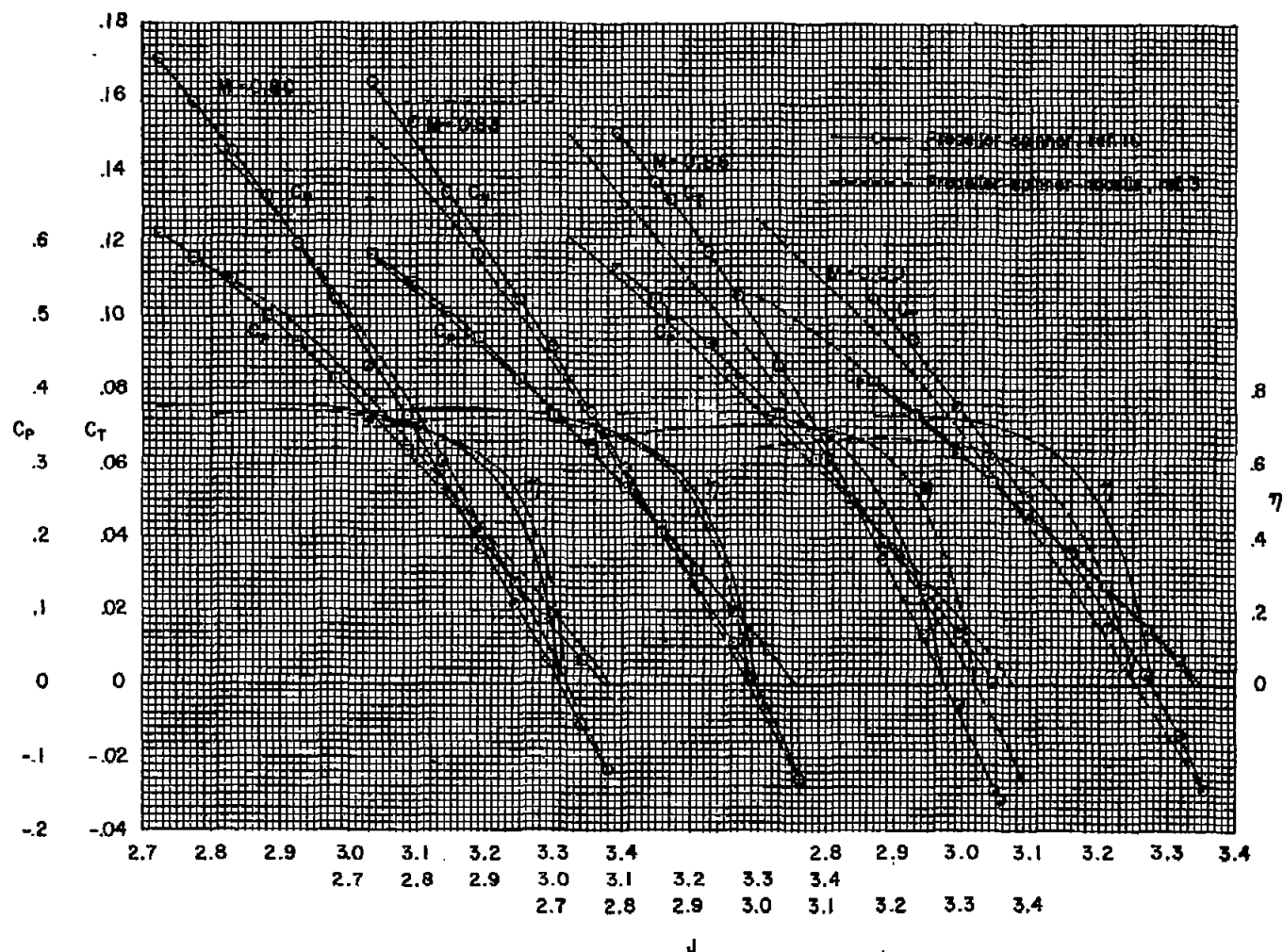


Figure 4.- The effect of the nacelle forebody on the characteristics of the sharp-trailing-edge propeller at several Mach numbers; $R = 1,600,000$, $\beta = 56^\circ$.

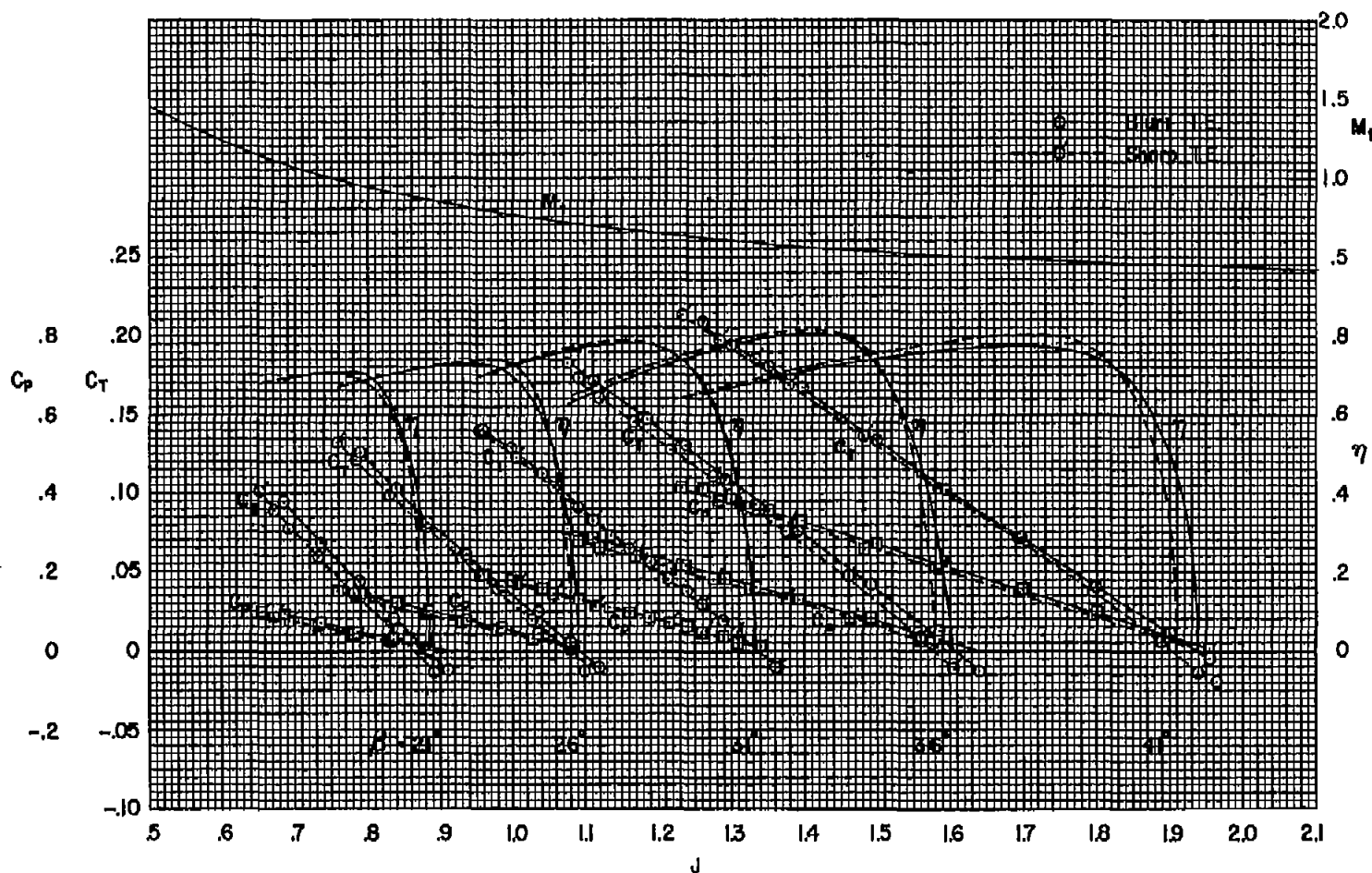
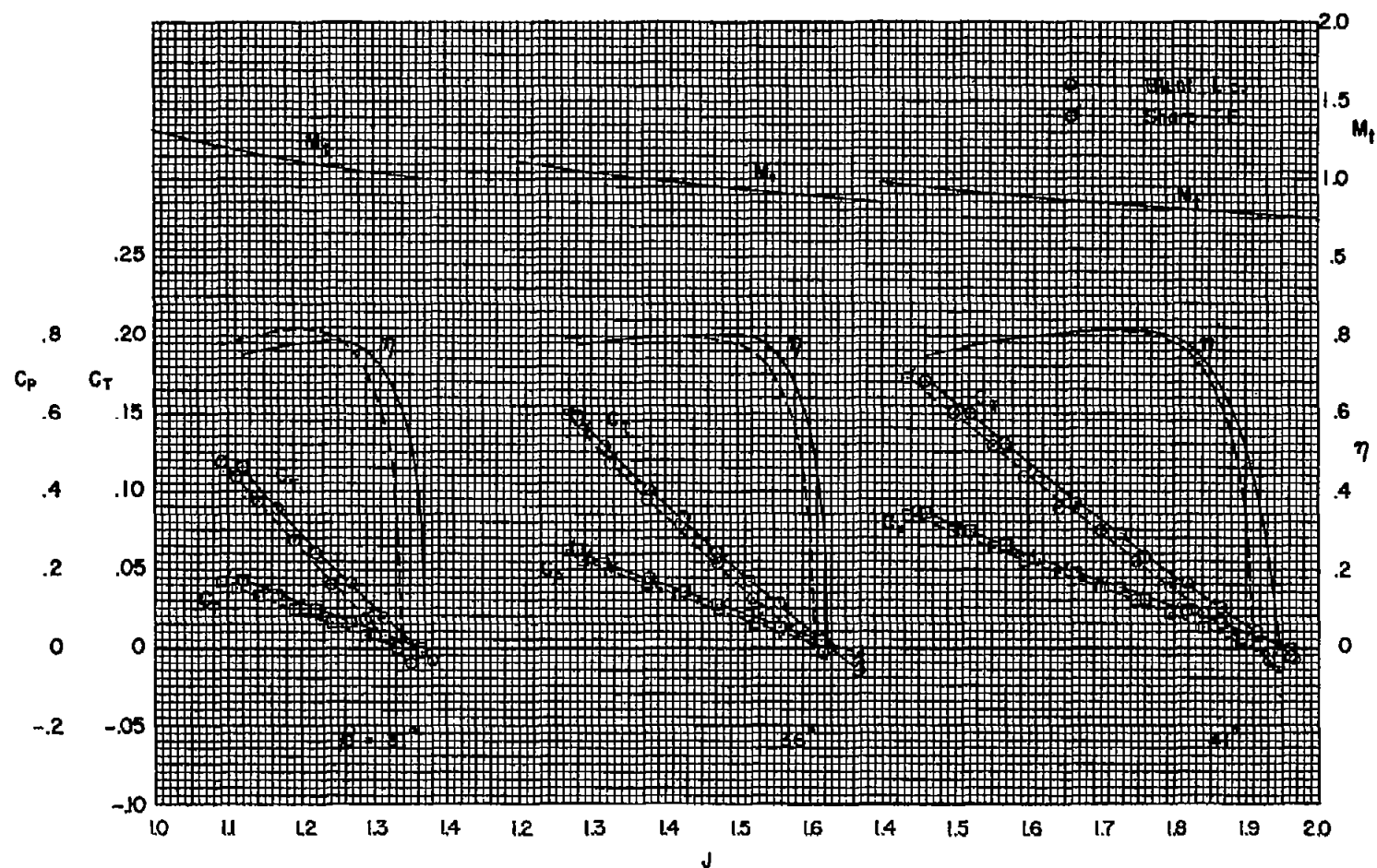
(a) $M = 0.24$

Figure 5.- The characteristics of the blunt- and sharp-trailing-edge propellers; $R = 1,600,000$.



(b) $M = 0.40$

Figure 5.- Continued.

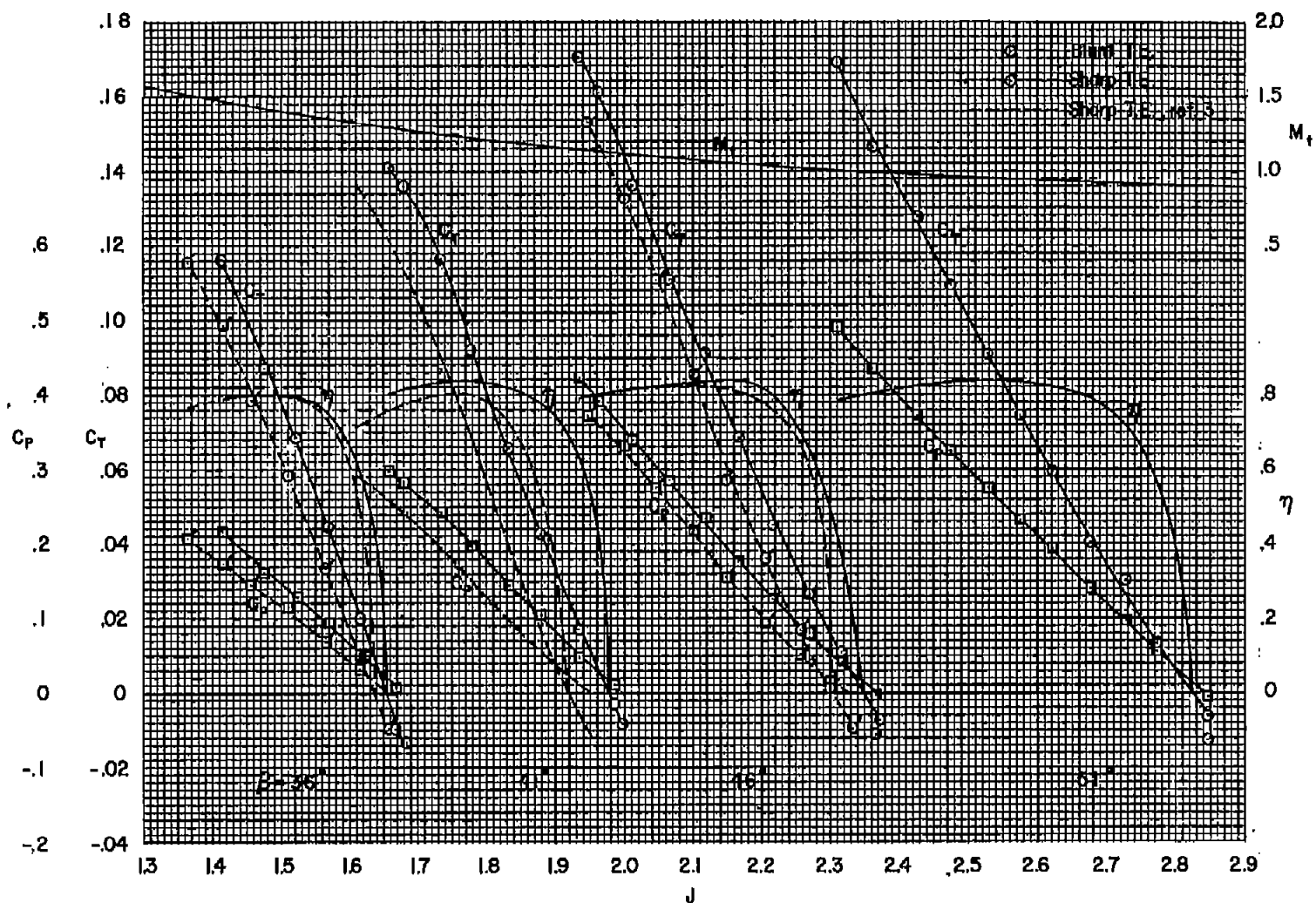
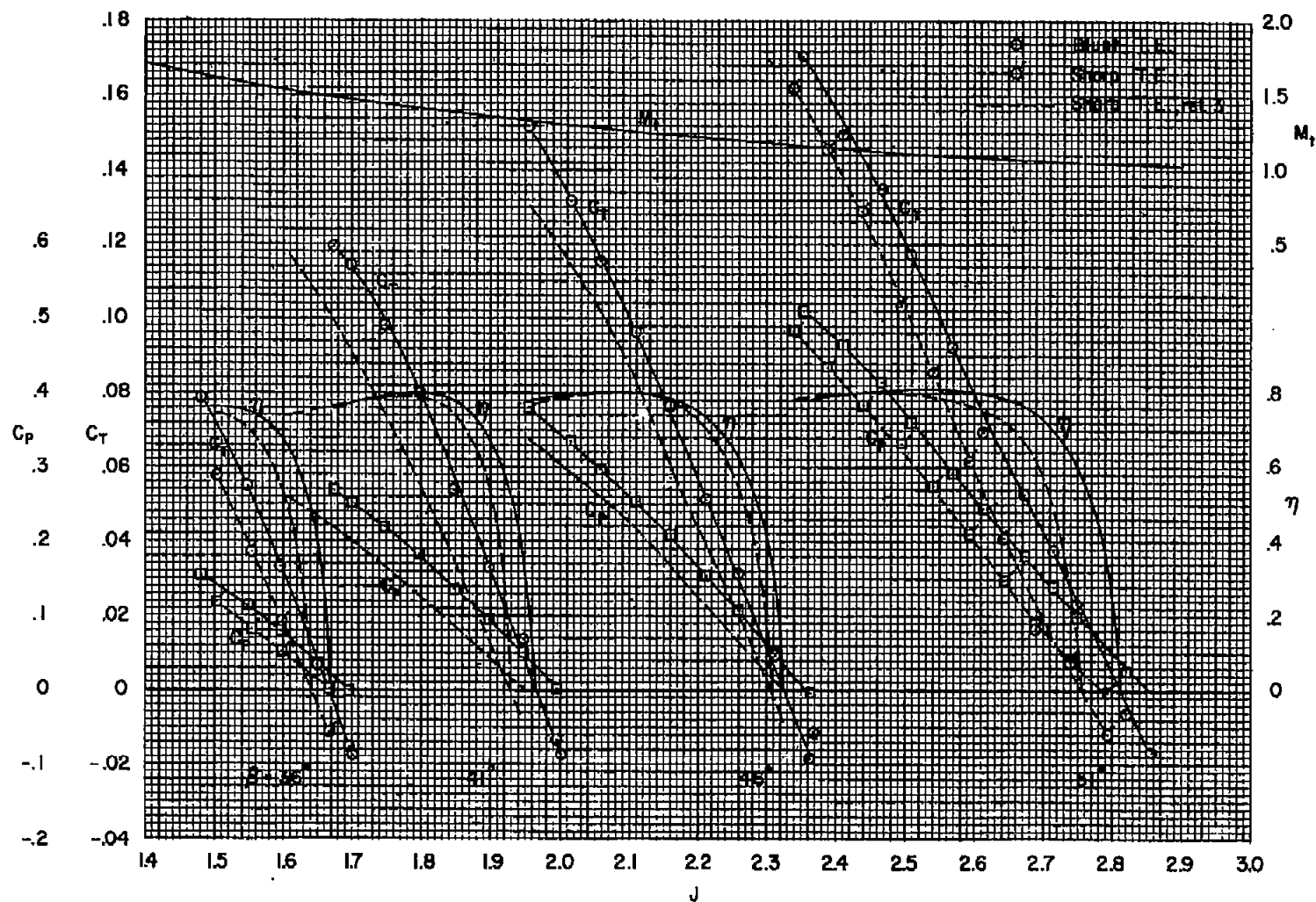
(c) $M = 0.60$

Figure 5.- Continued.



(d) $M = 0.70$

Figure 5.- Continued.

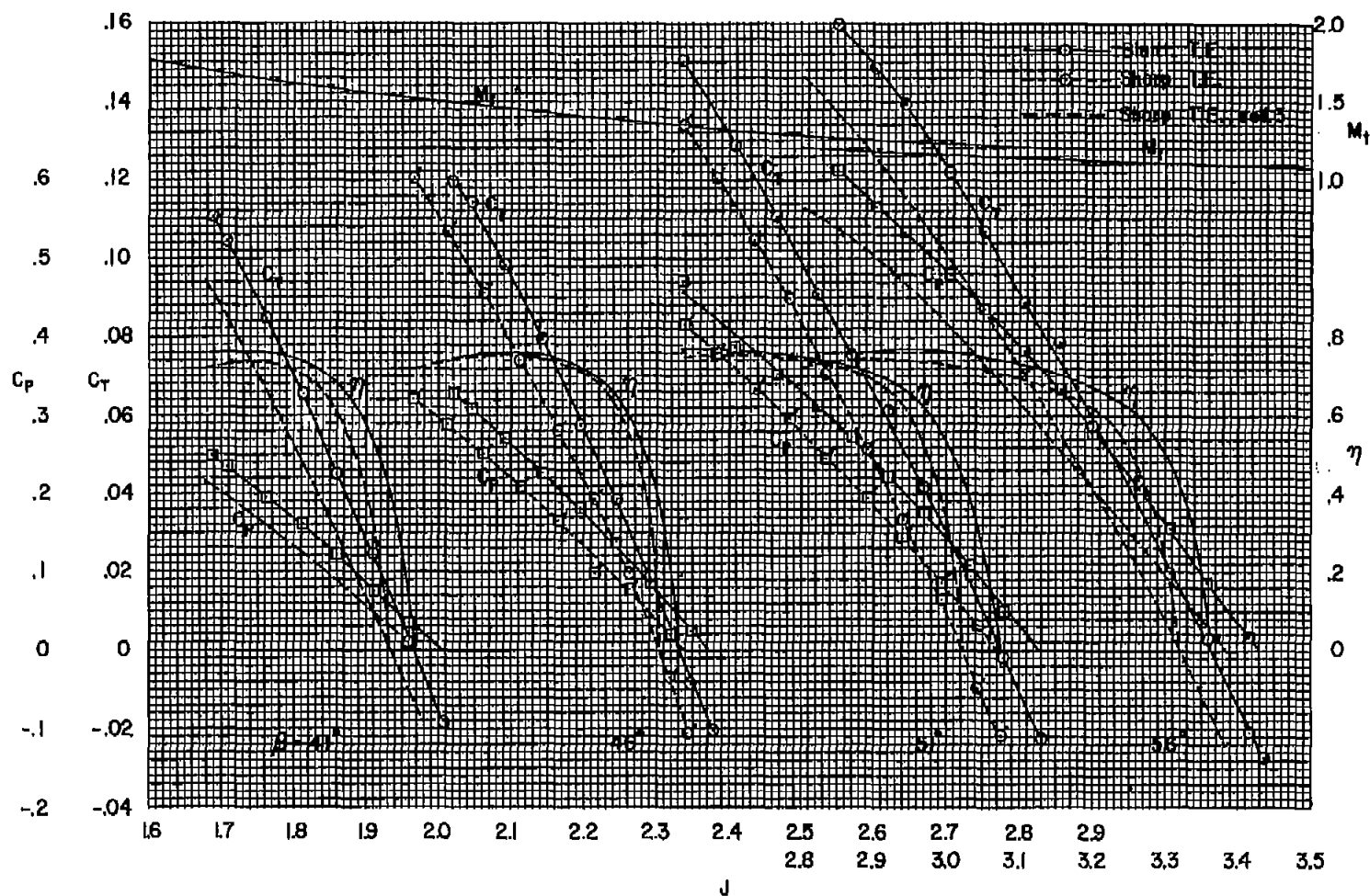
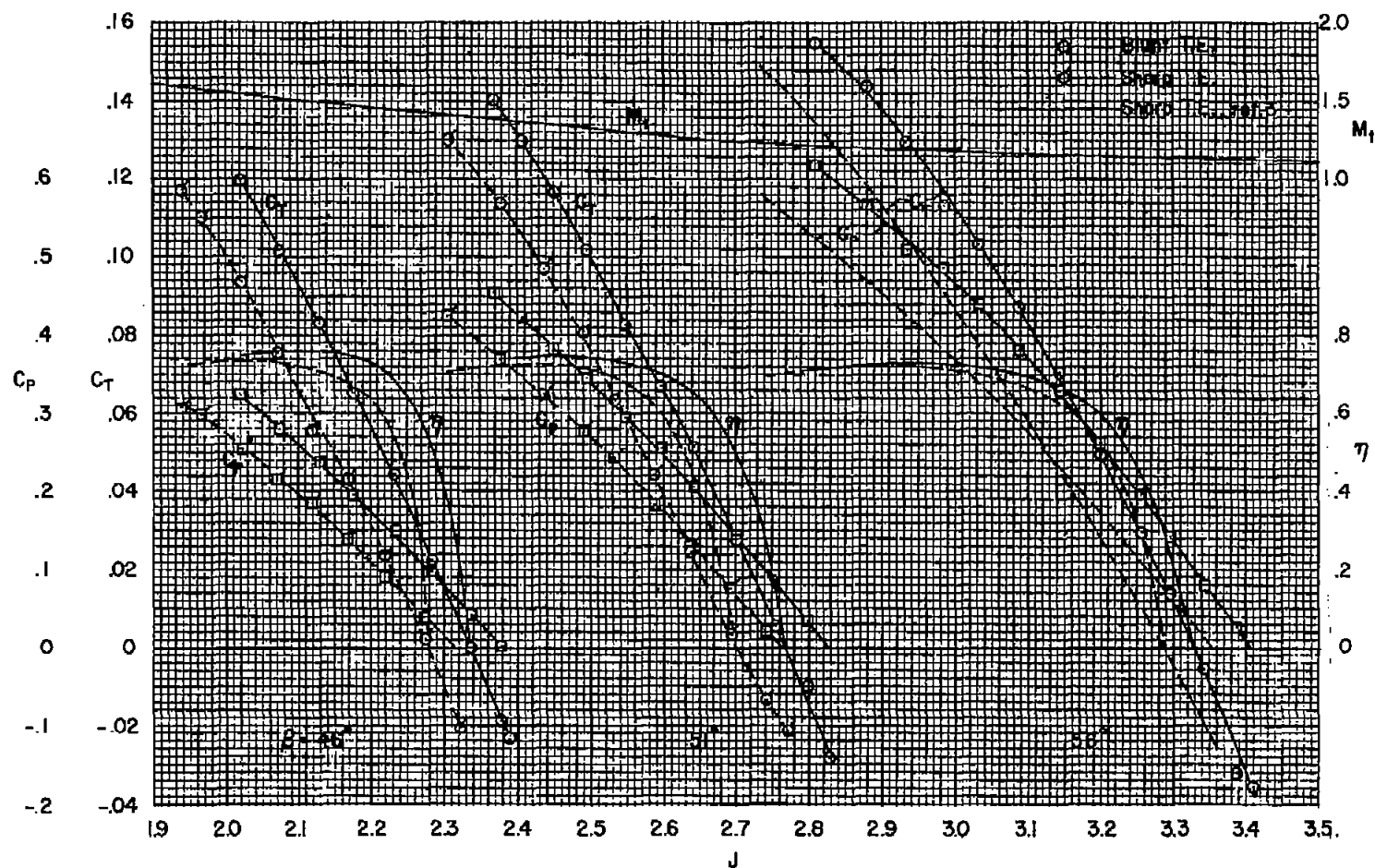
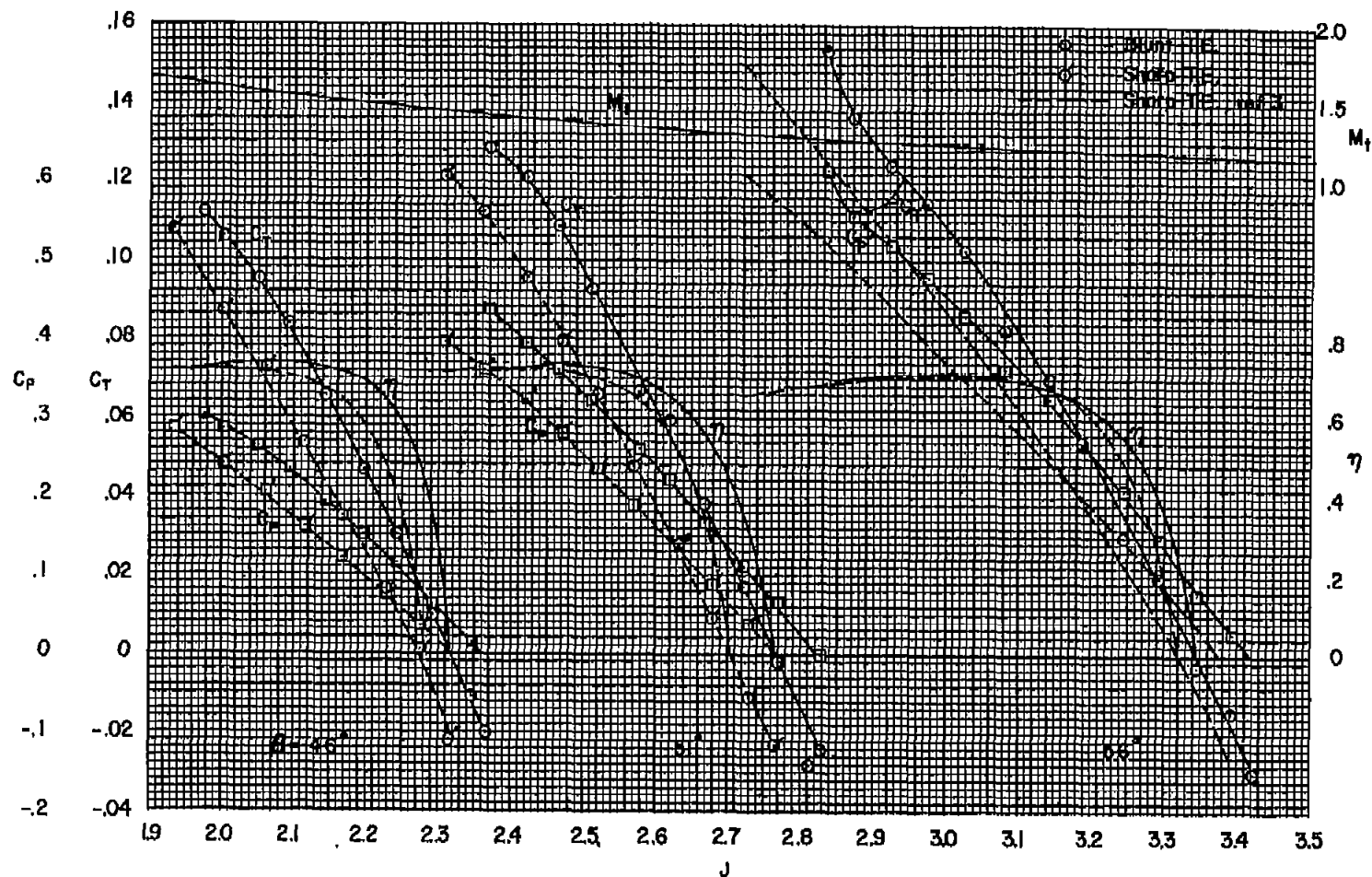
(e) $M = 0.80$

Figure 5.- Continued.



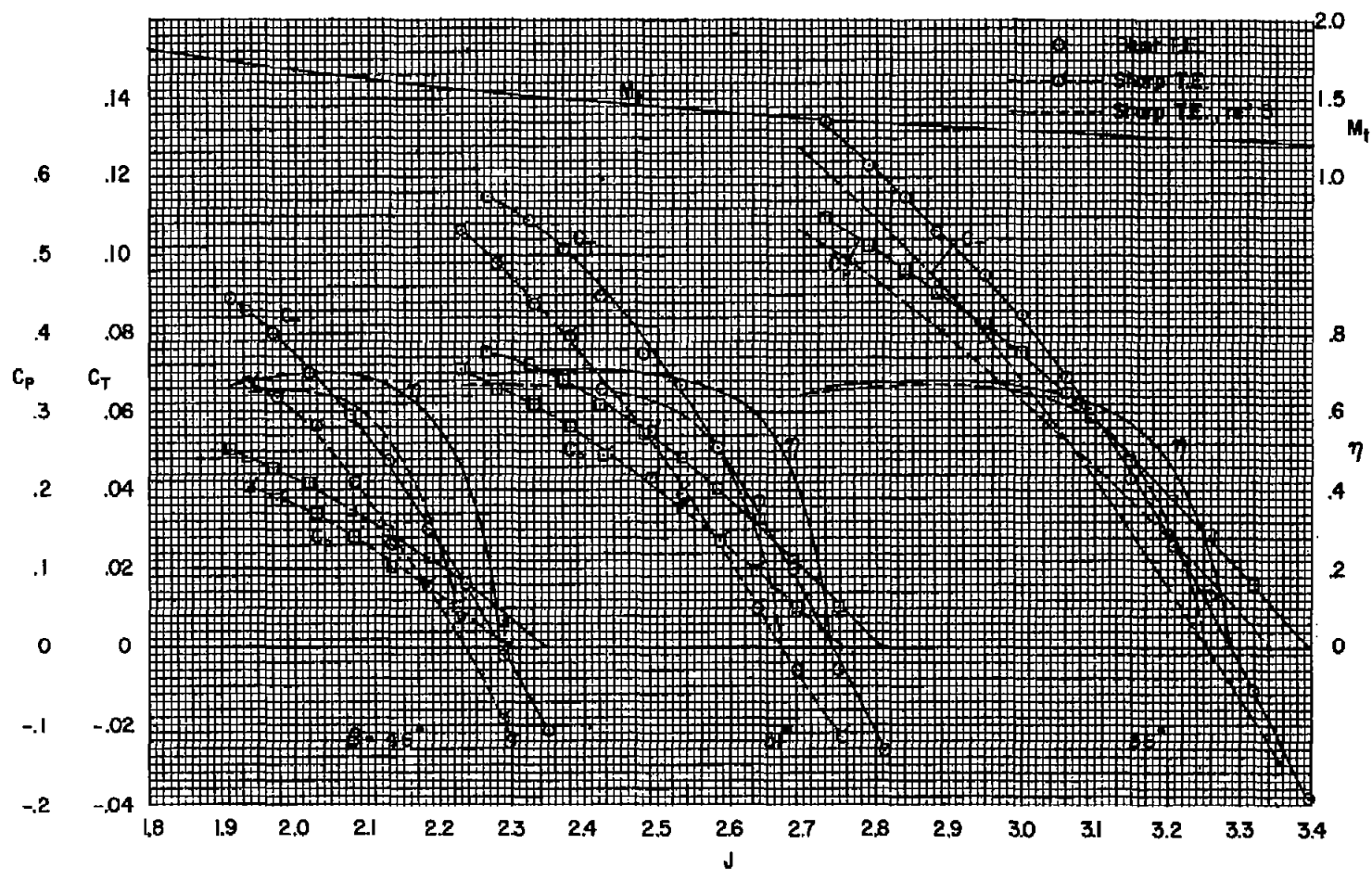
(f) $M = 0.83$

Figure 5.- Continued.



(g) $M = 0.86$

Figure 5.- Continued.



(h) $M = 0.90$

Figure 5.- Continued.

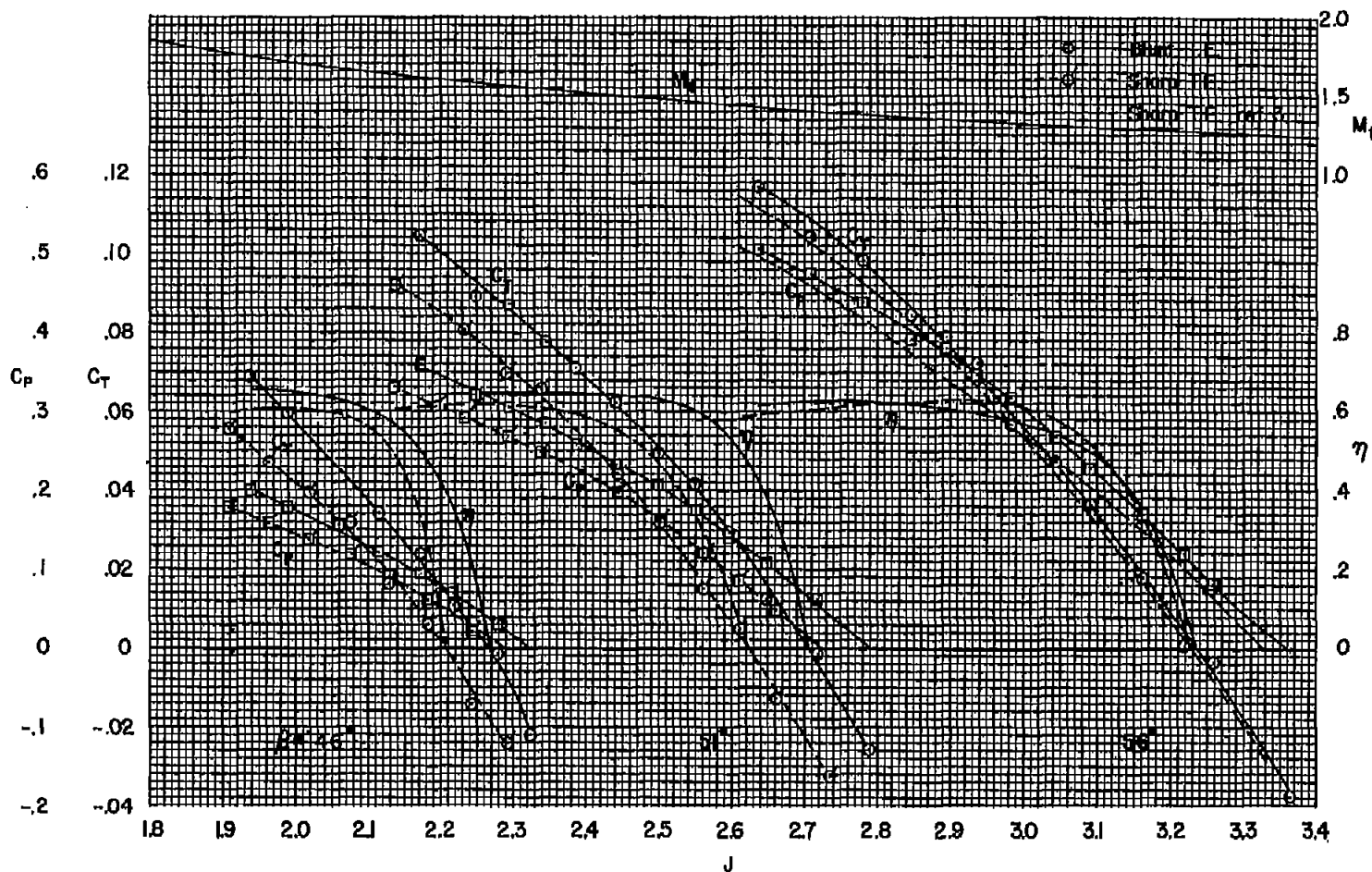
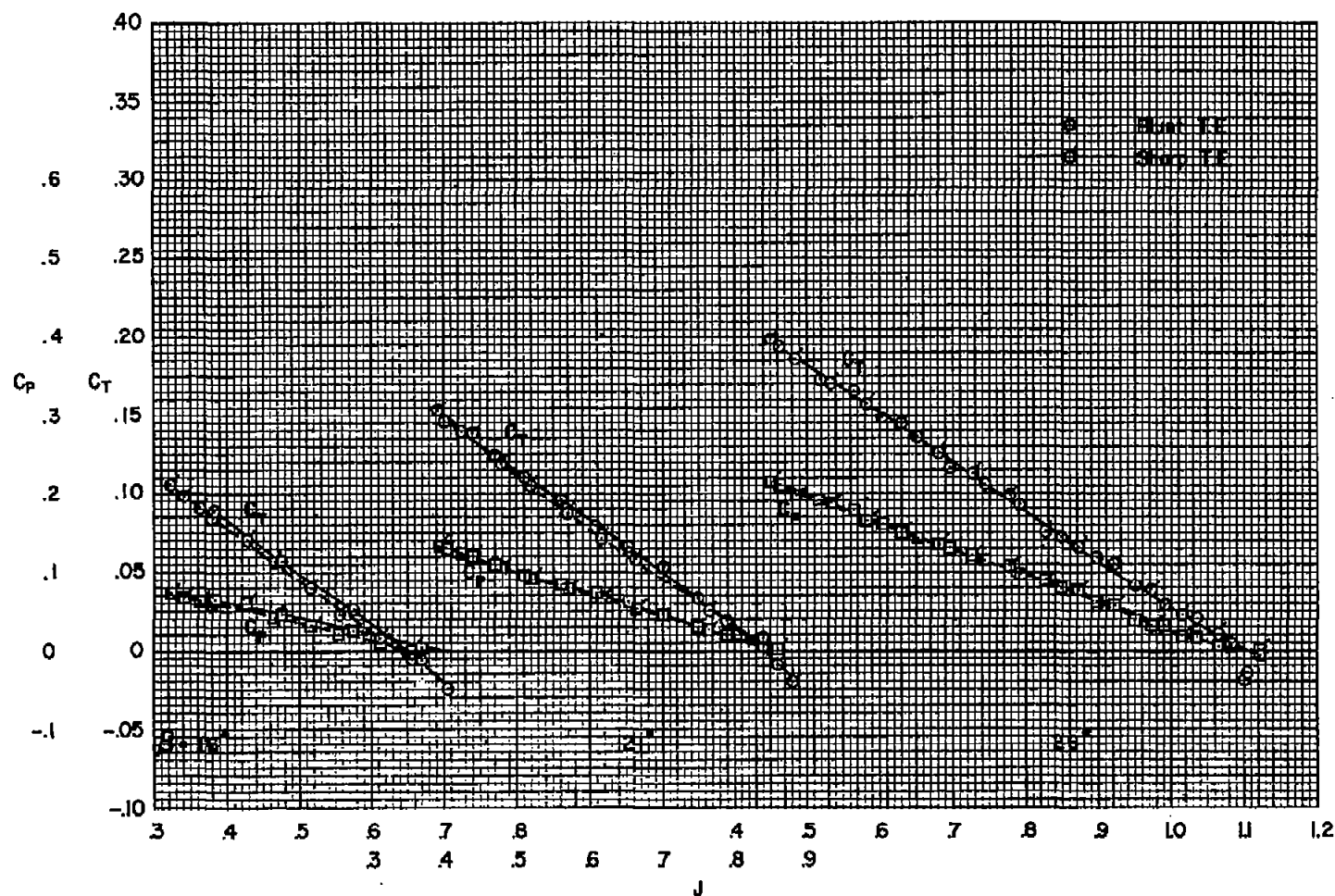
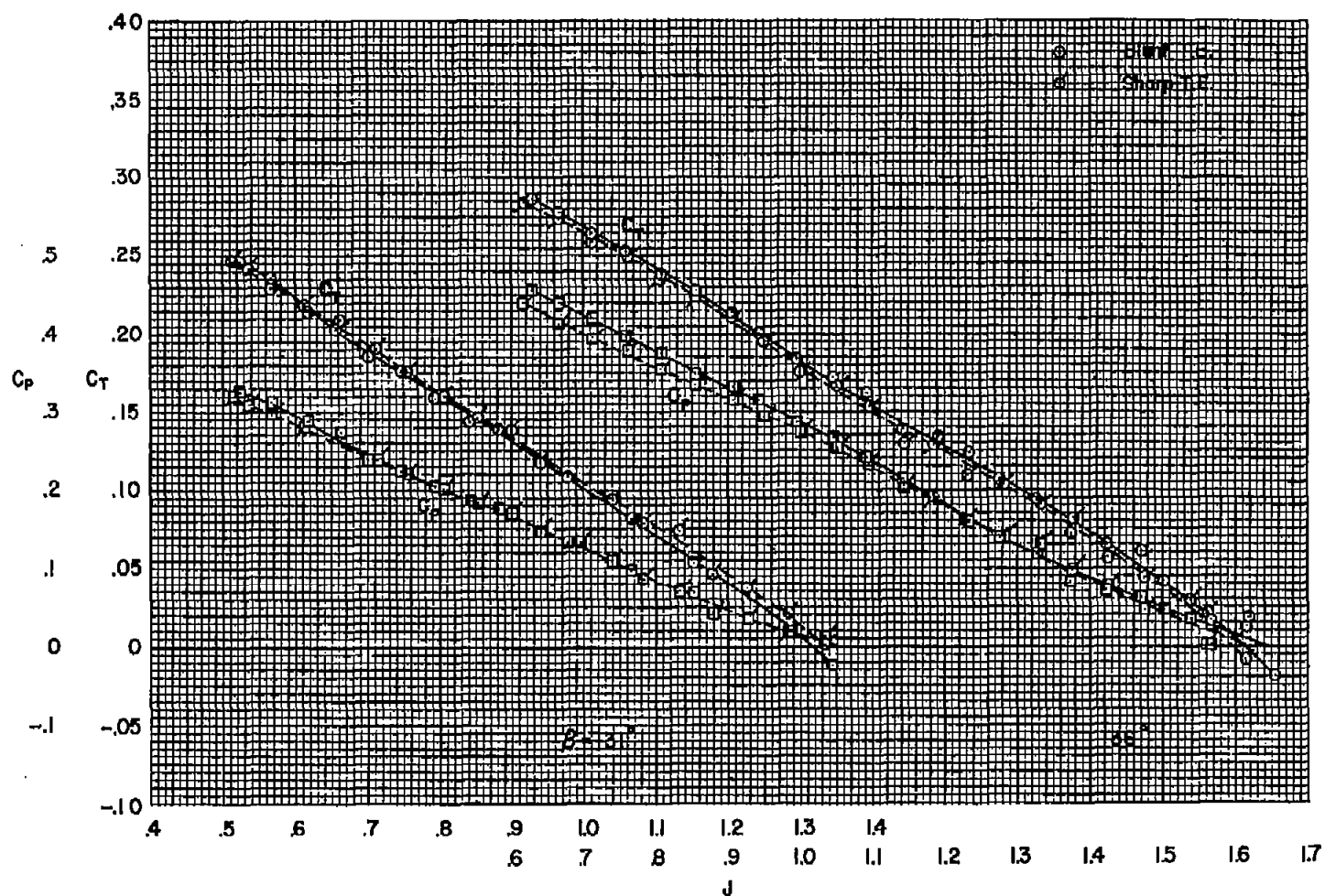
(i) $M = 0.92$

Figure 5.- Concluded.



(a) $\beta = 16^\circ, 21^\circ, 26^\circ$

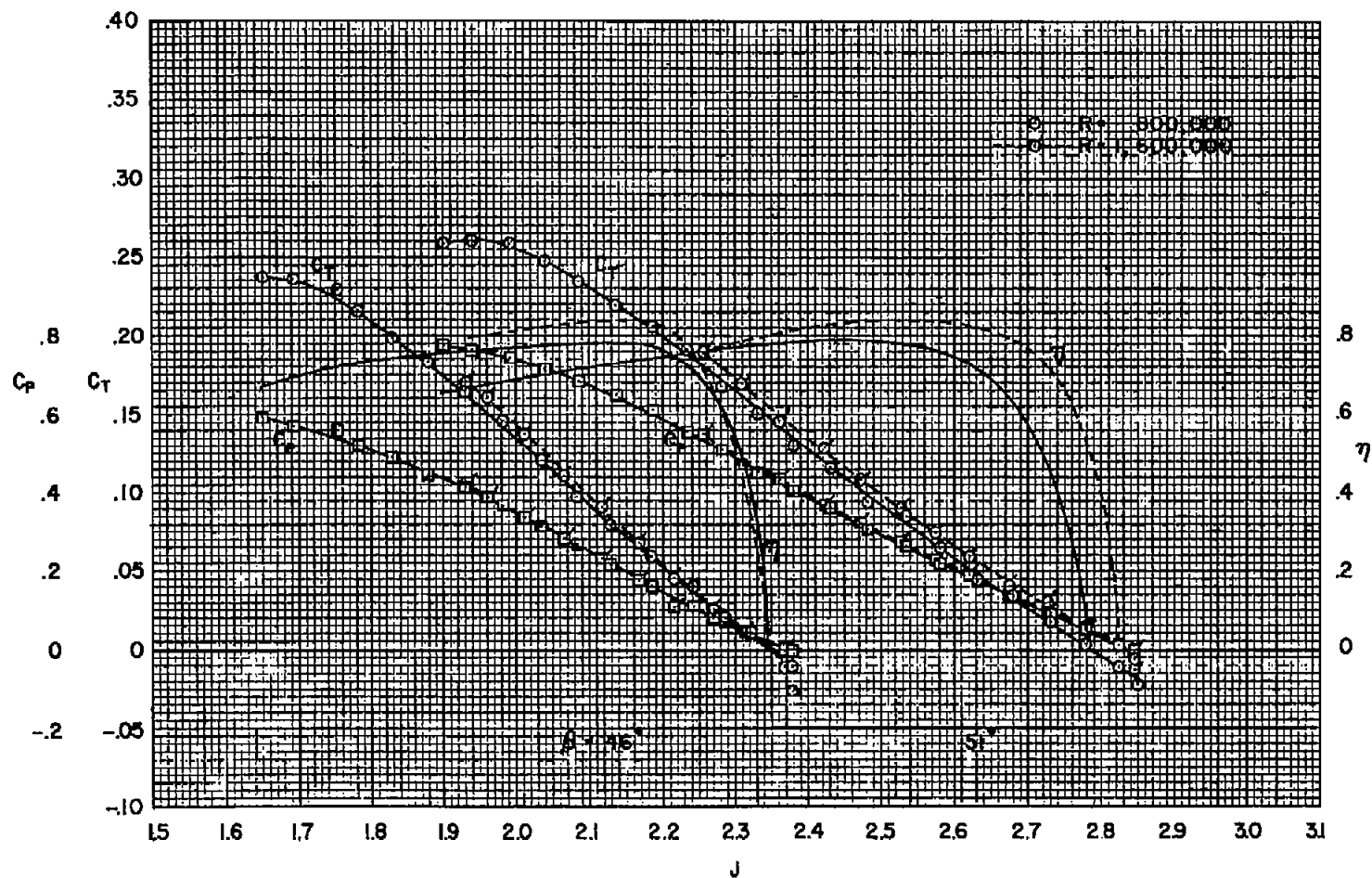
Figure 6.- The characteristics of the blunt- and sharp-trailing-edge propellers; $R = 1,150,000$, $M = 0.082$.



(b) $\beta = 31^\circ, 36^\circ$

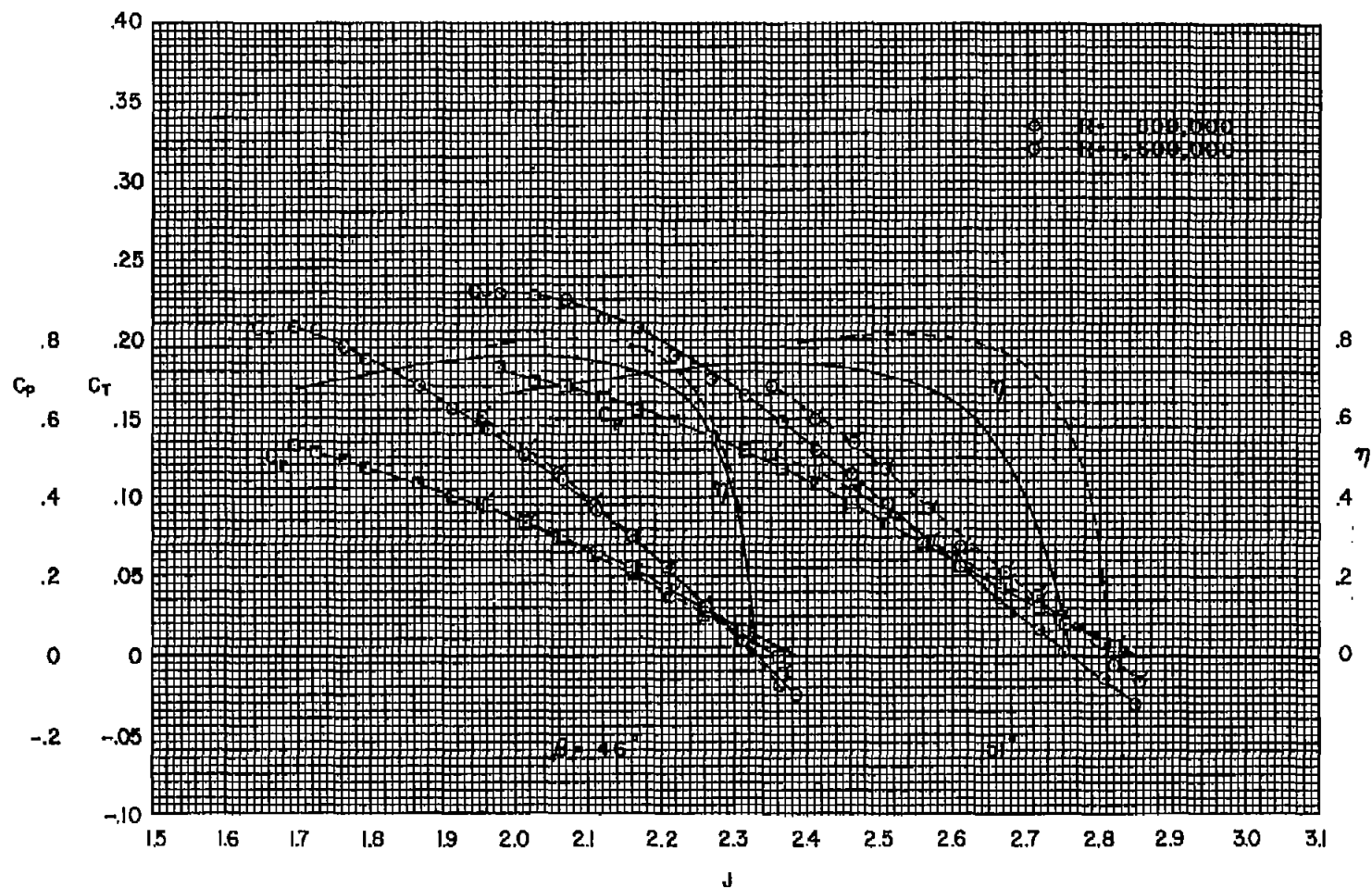
Figure 6.- Concluded.

CONFIDENTIAL



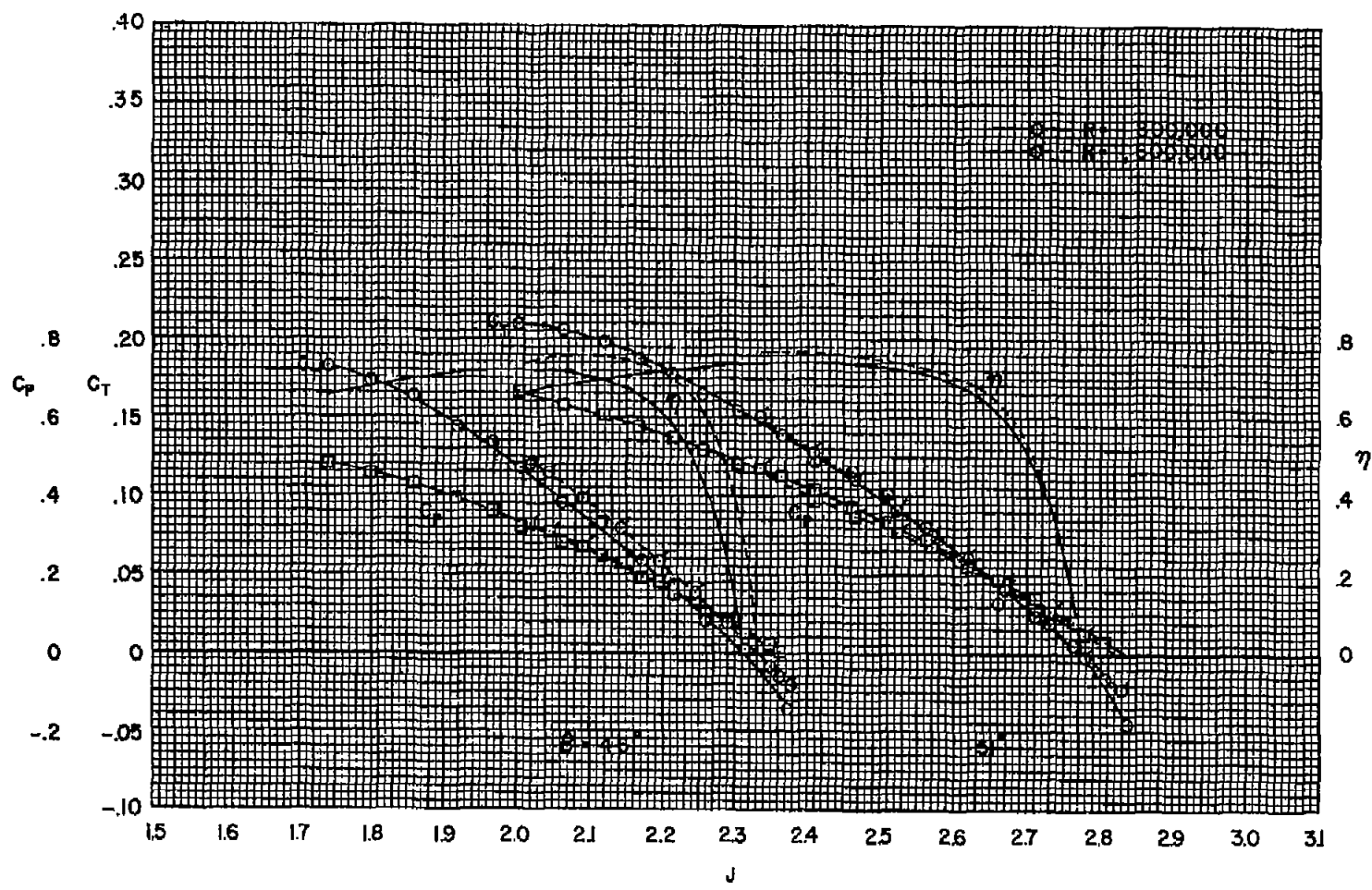
(a) $M = 0.60$

Figure 7.- The effect of Reynolds number on the characteristics of the blunt-trailing-edge propeller.



(b) $M = 0.70$

Figure 7.- Continued.



(c) $M = 0.80$

Figure 7.- Continued.

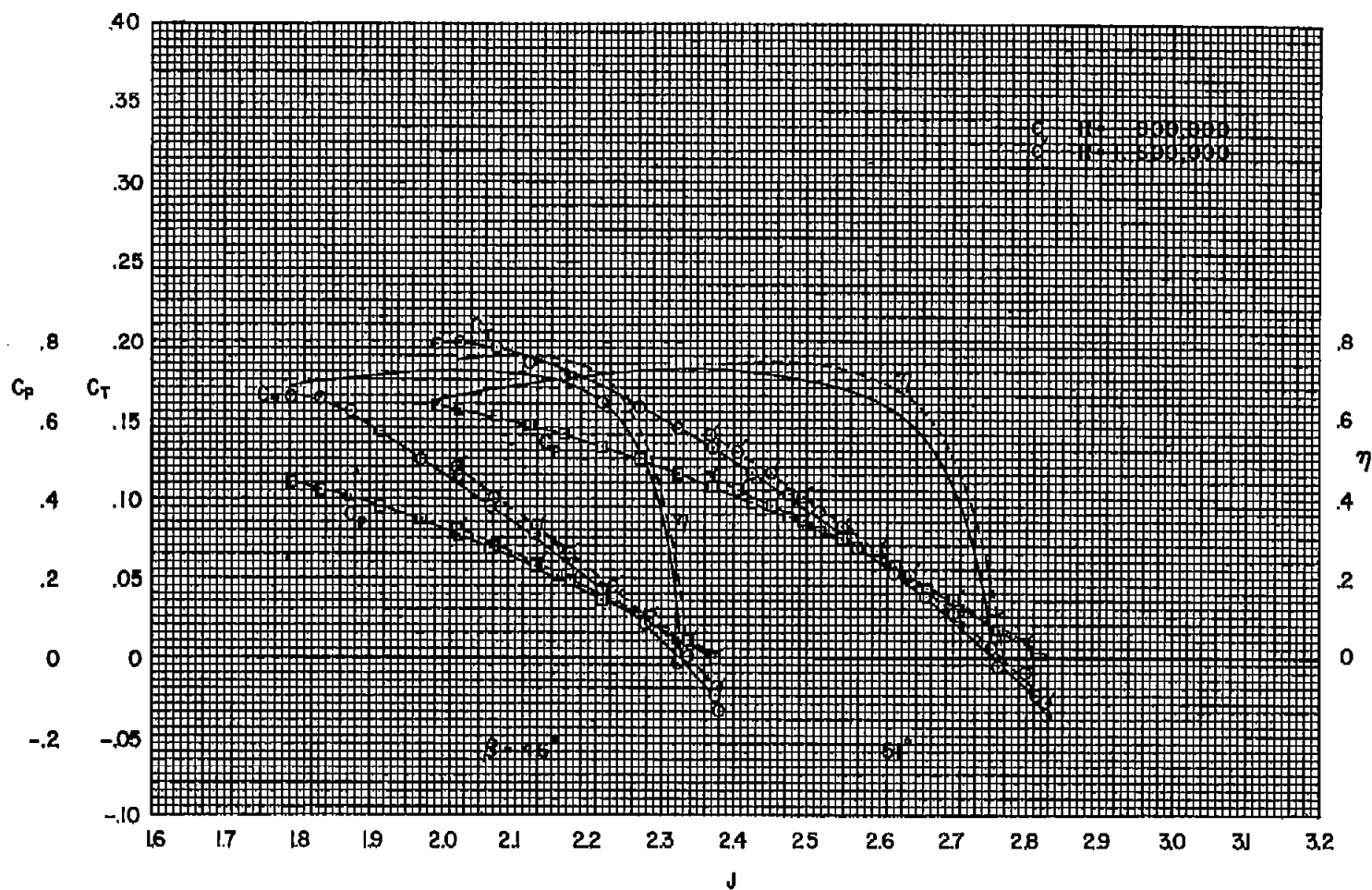
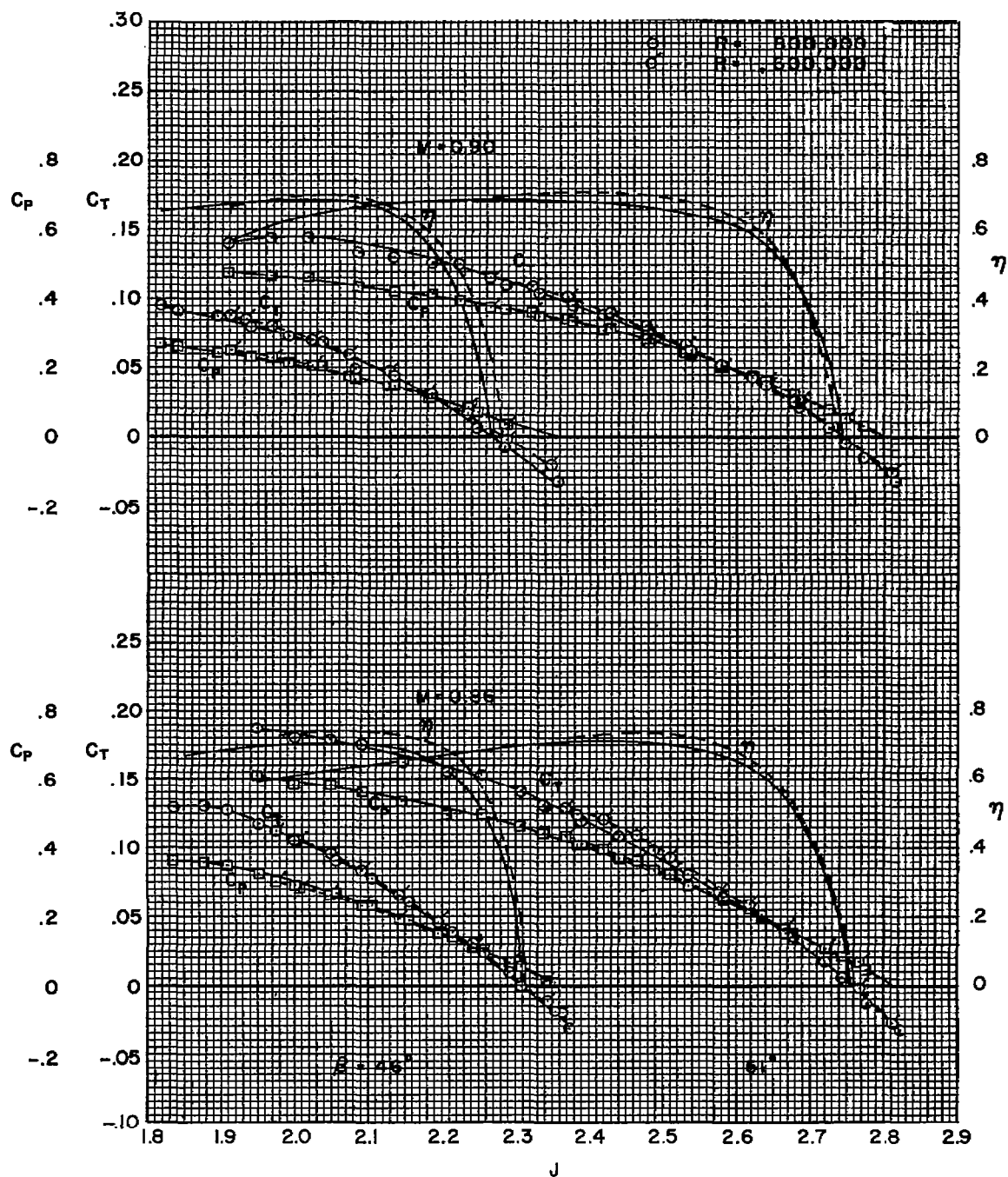
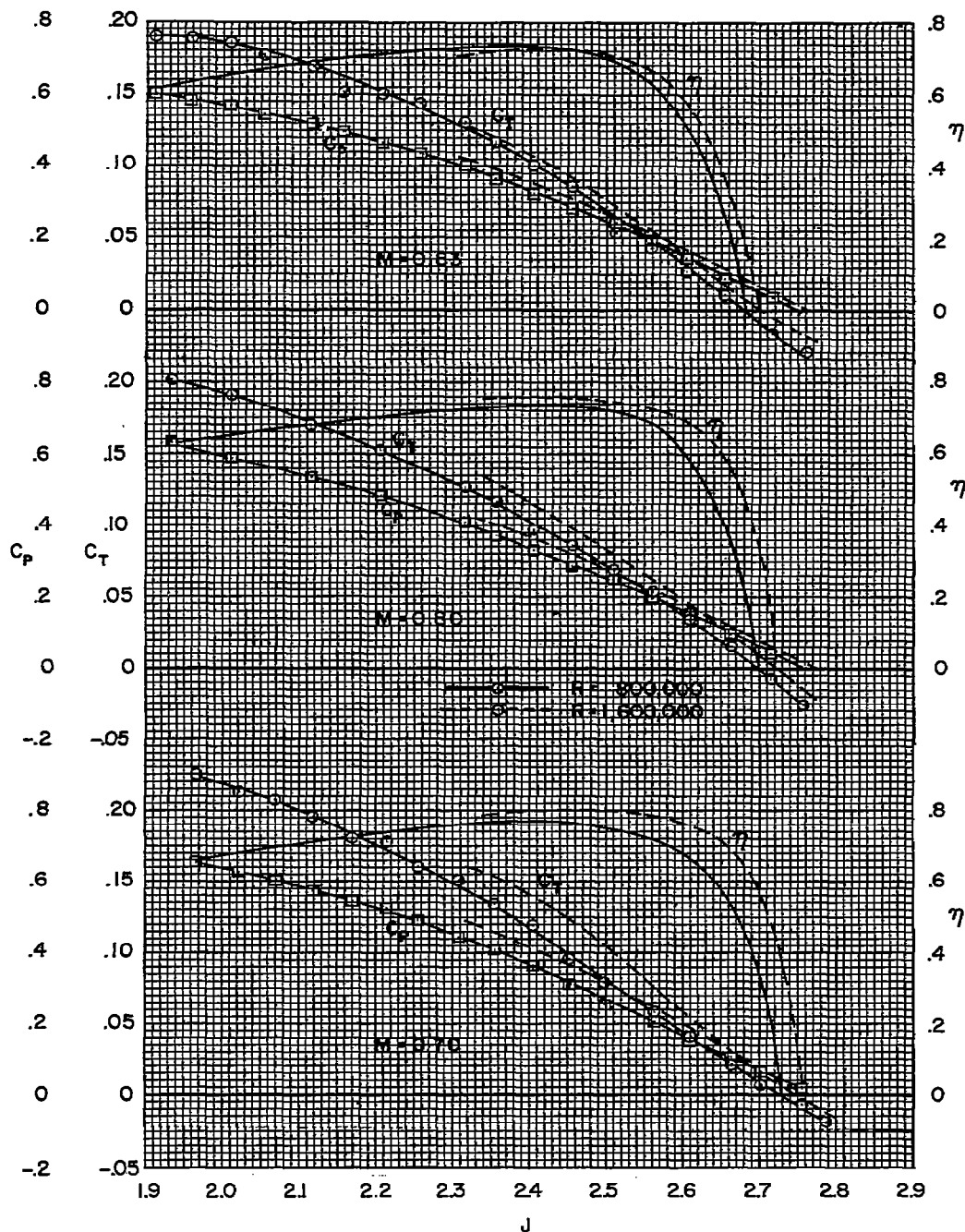
(d) $M = 0.83$

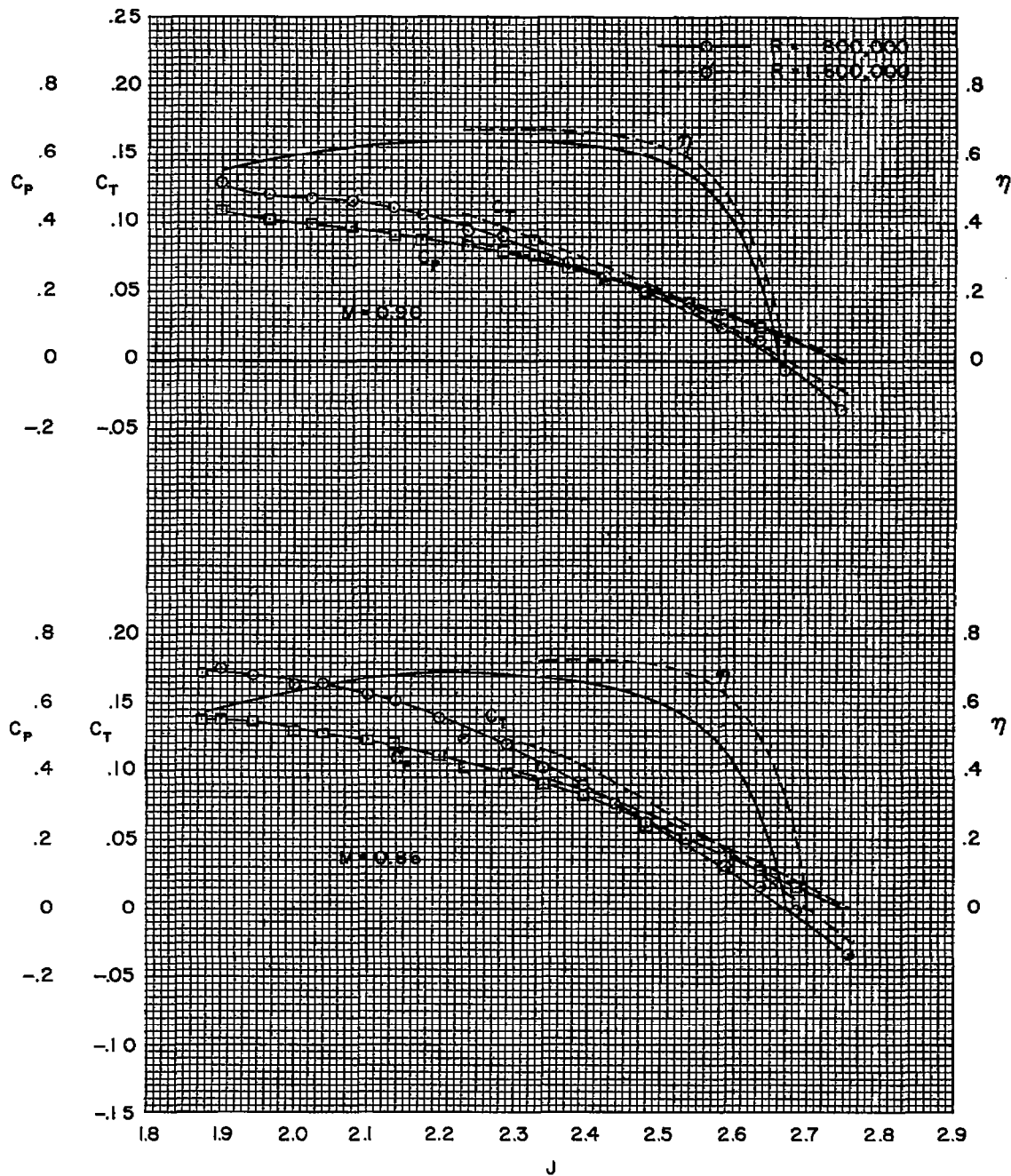
Figure 7.- Continued.



(e) $M = 0.86, 0.90$

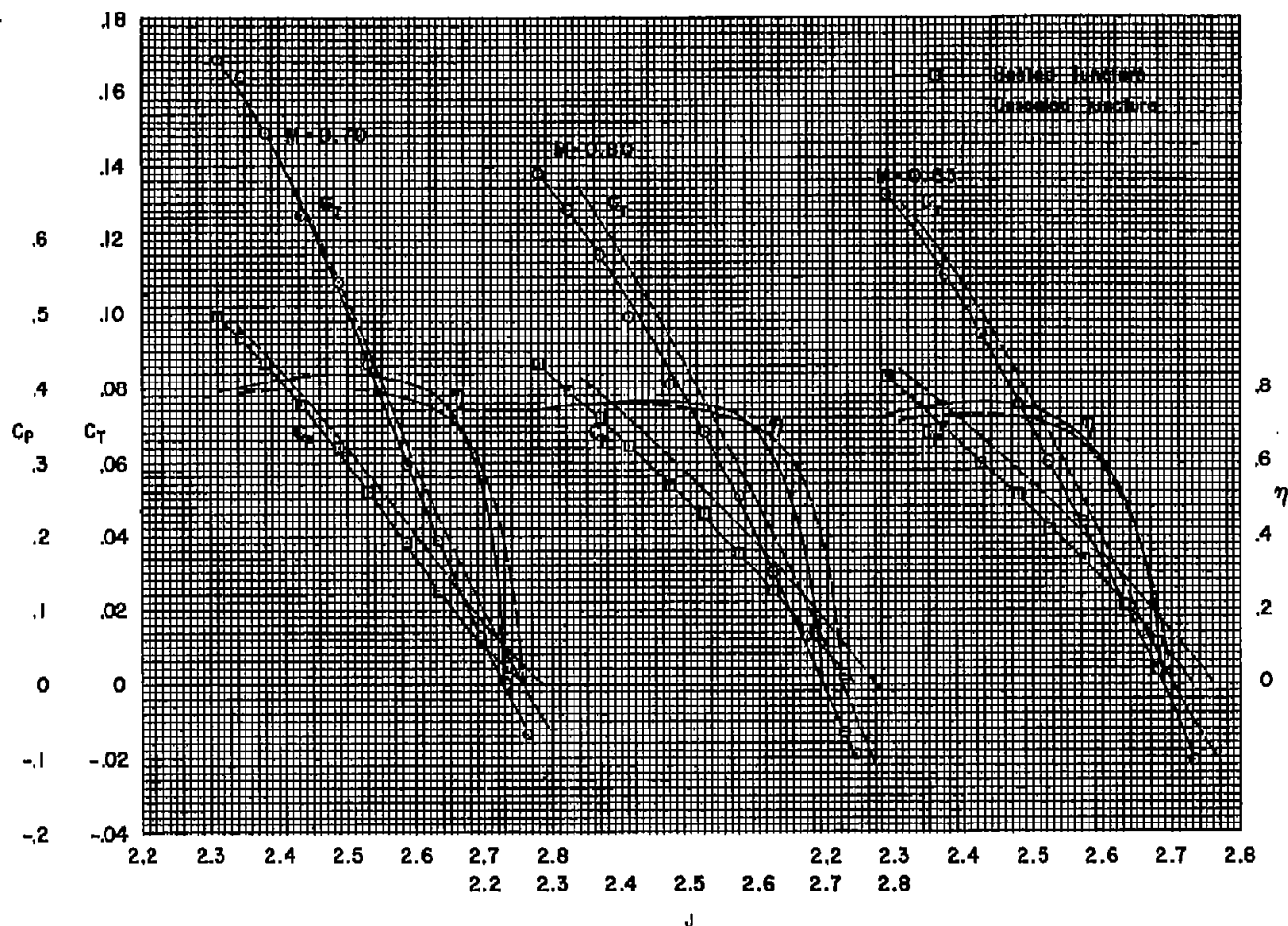
Figure 7.- Concluded.

(a) $M = 0.70, 0.80, 0.83$ Figure 8.- The effect of Reynolds number on the characteristics of the sharp-trailing-edge propellers; $\beta = 51^\circ$.



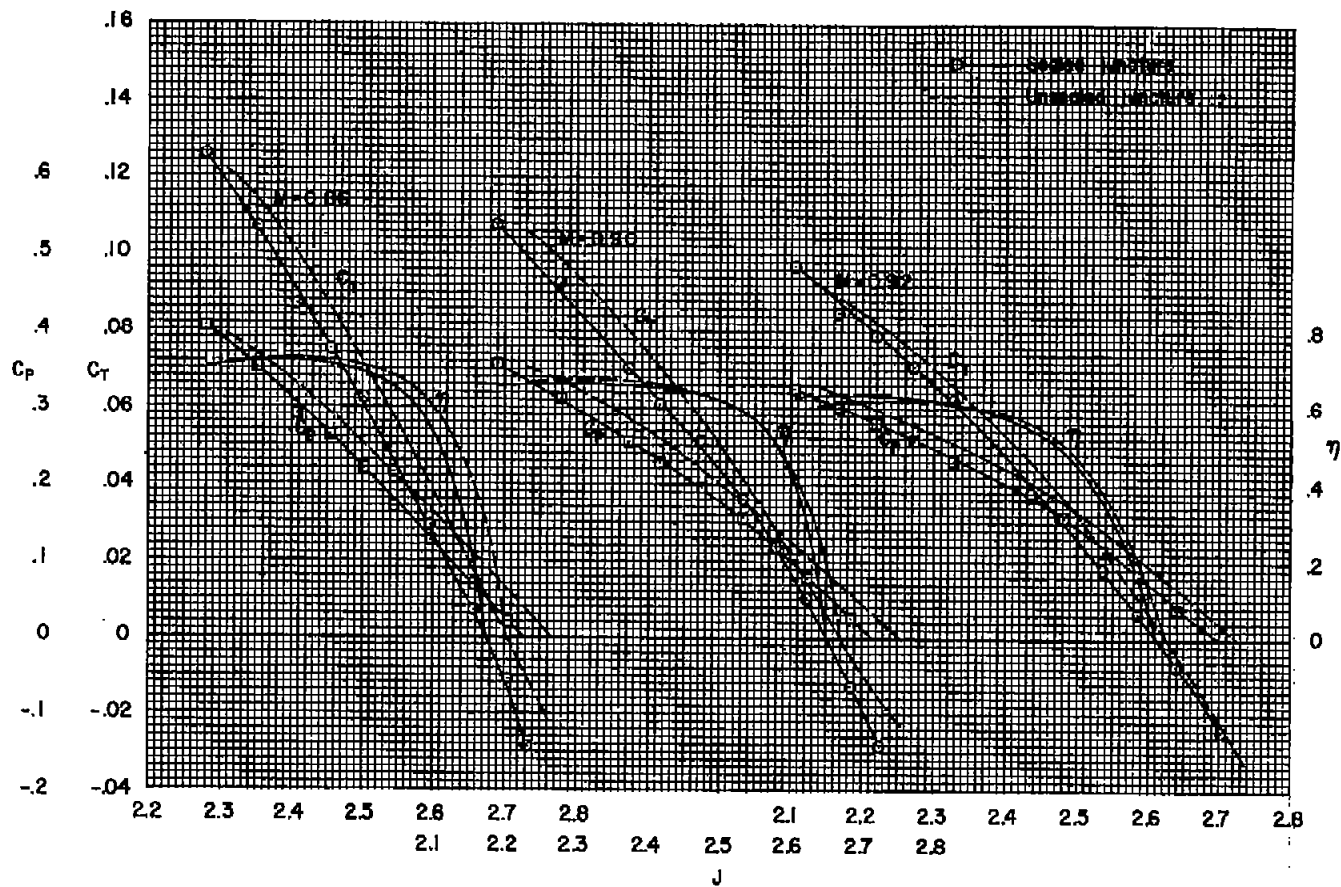
(b) $M = 0.86, 0.90$

Figure 8.- Concluded.



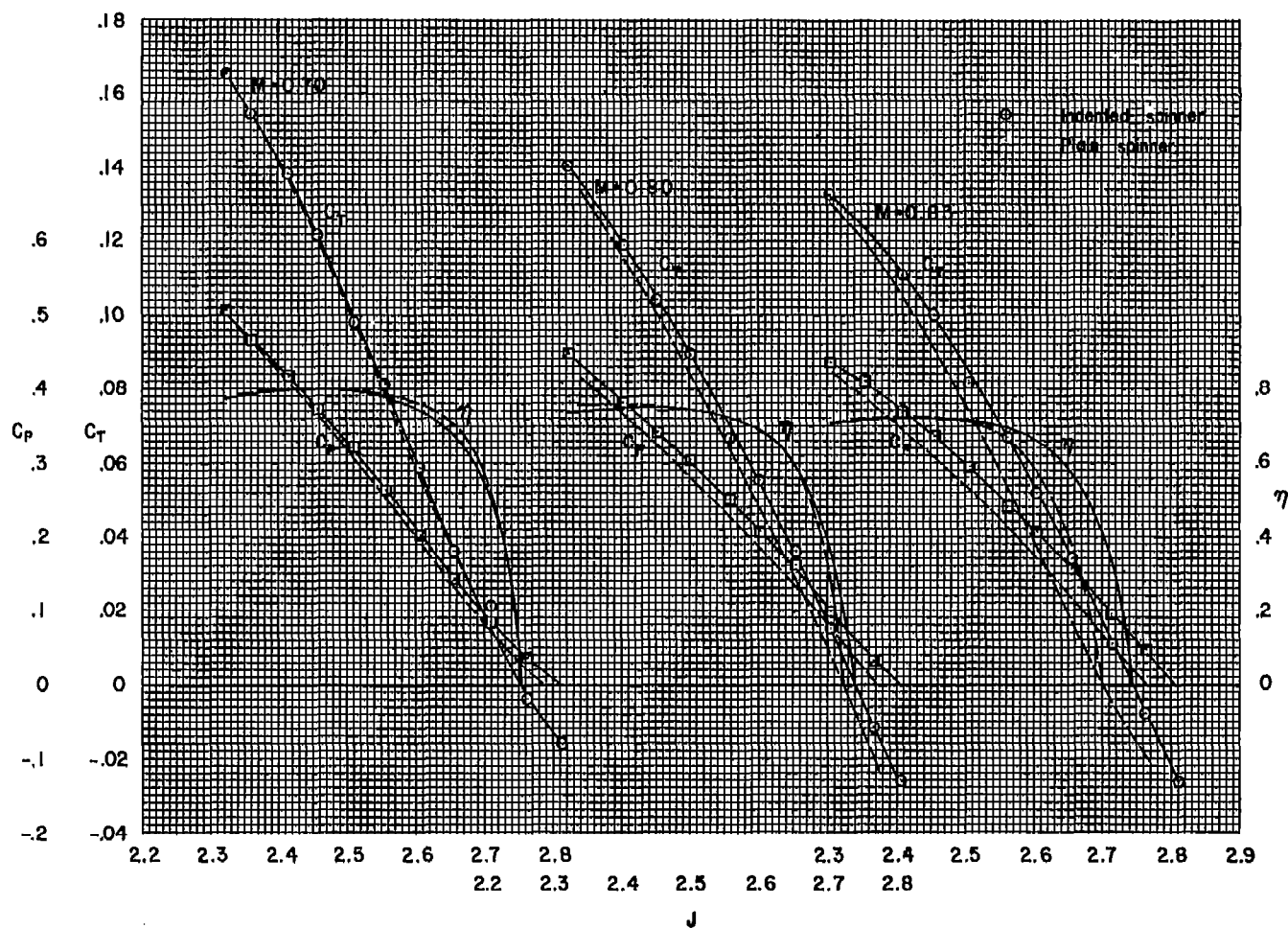
(a) $M = 0.70, 0.80, 0.83$

Figure 9.- The effect of sealing the blade-spinner juncture on the characteristics of the sharp-trailing-edge propeller; $R = 1,600,000$, $\beta = 51^\circ$.



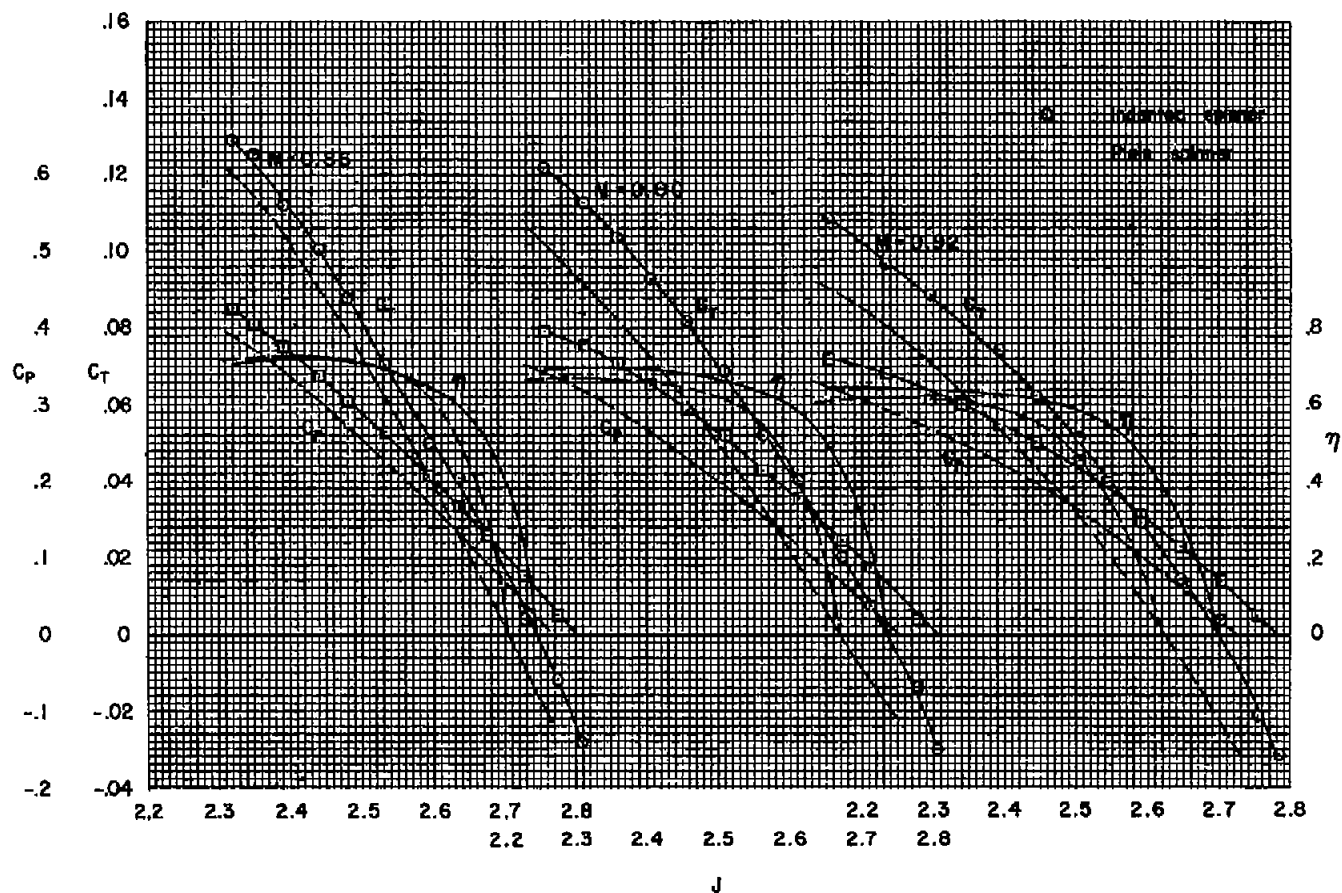
(b) $M = 0.86, 0.90, 0.92$

Figure 9.- Concluded.



(a) $M = 0.70, 0.80, 0.83$

Figure 10.- The effect of spinner indentation on the characteristics of the sharp-trailing-edge propeller; $R = 1,600,000$, $\beta = 51^\circ$.



(b) $M = 0.86, 0.90, 0.92$

Figure 10.- Concluded.

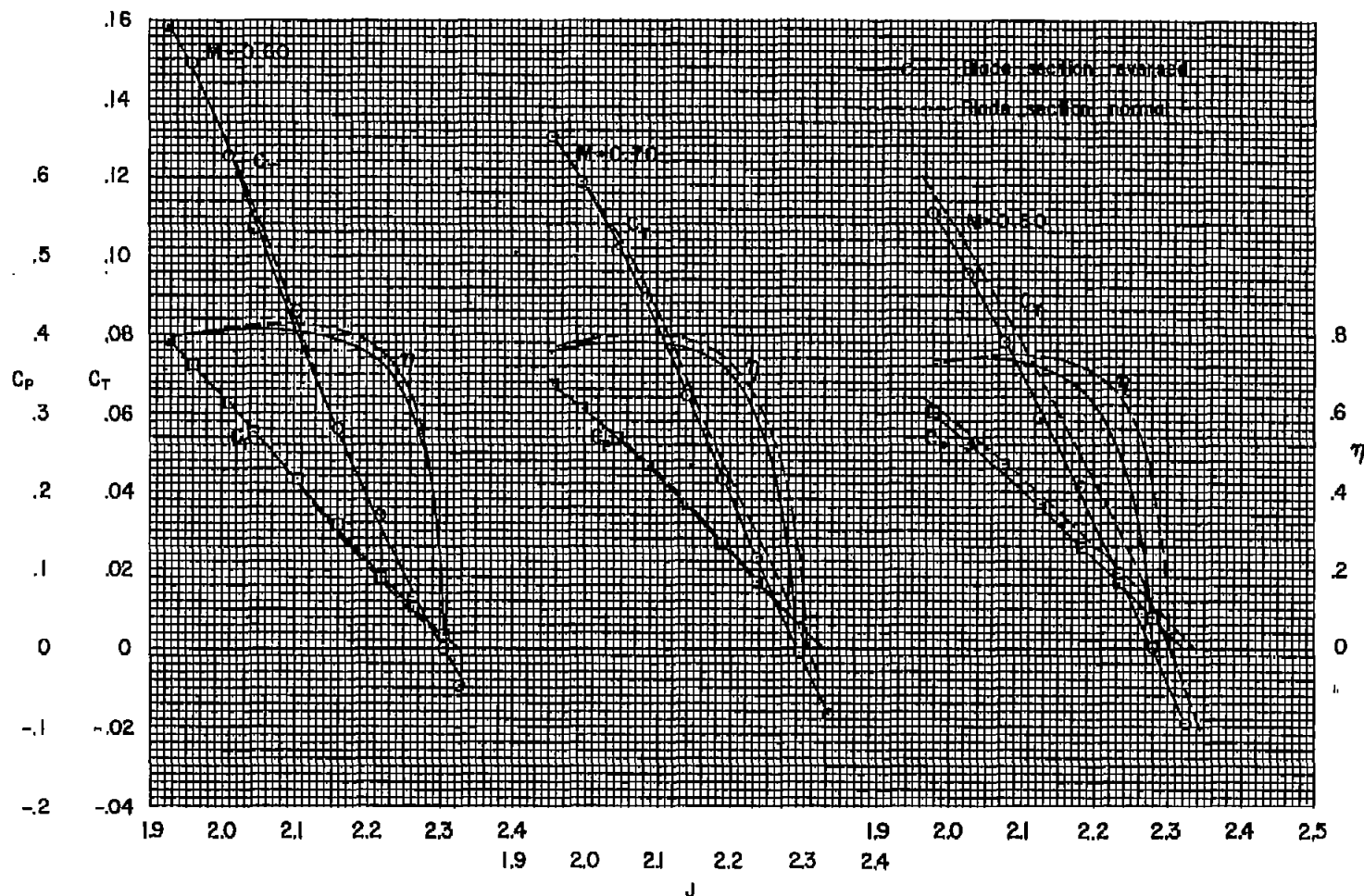
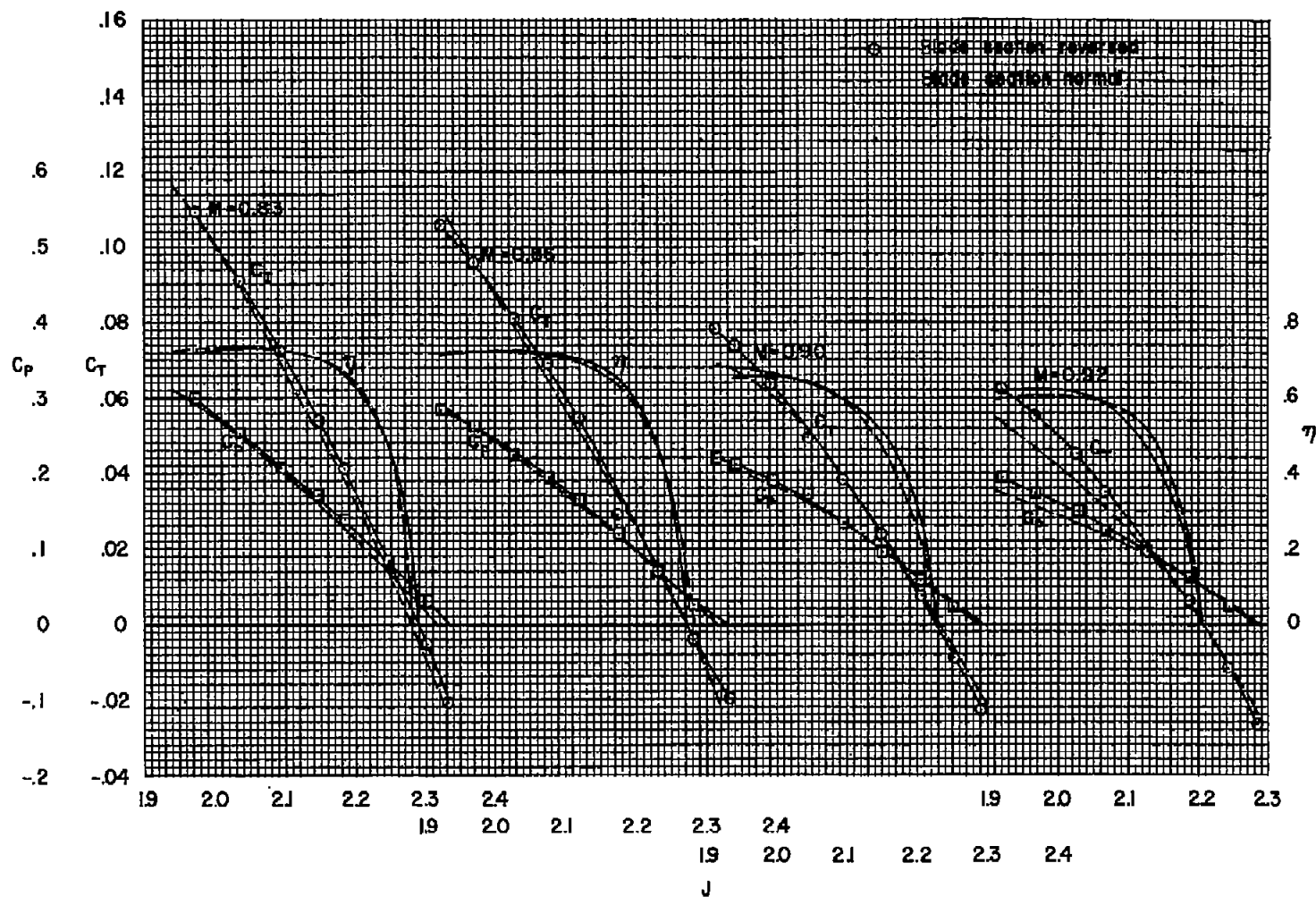
(a) $M = 0.60, 0.70, 0.80$

Figure 11.- The effect of reversed blade section on the characteristics of the sharp-trailing-edge propeller; $R = 1,600,000$, $\beta = 46^\circ$.



(b) $M = 0.83, 0.86, 0.90, 0.92$

Figure 11.- Concluded.

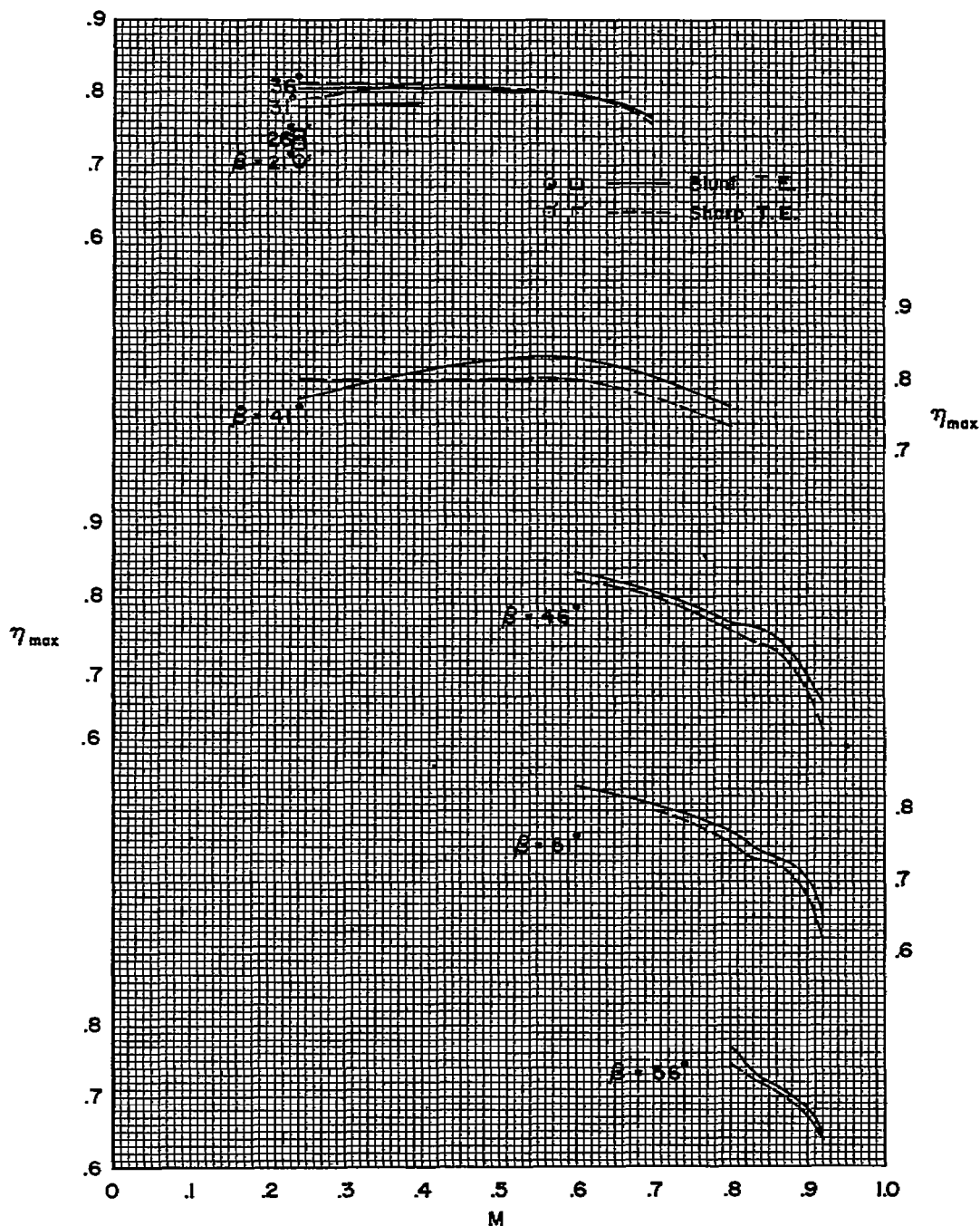


Figure 12.- The effect of forward Mach number on the maximum efficiency of the blunt- and sharp-trailing-edge propellers; $R = 1,600,000$.

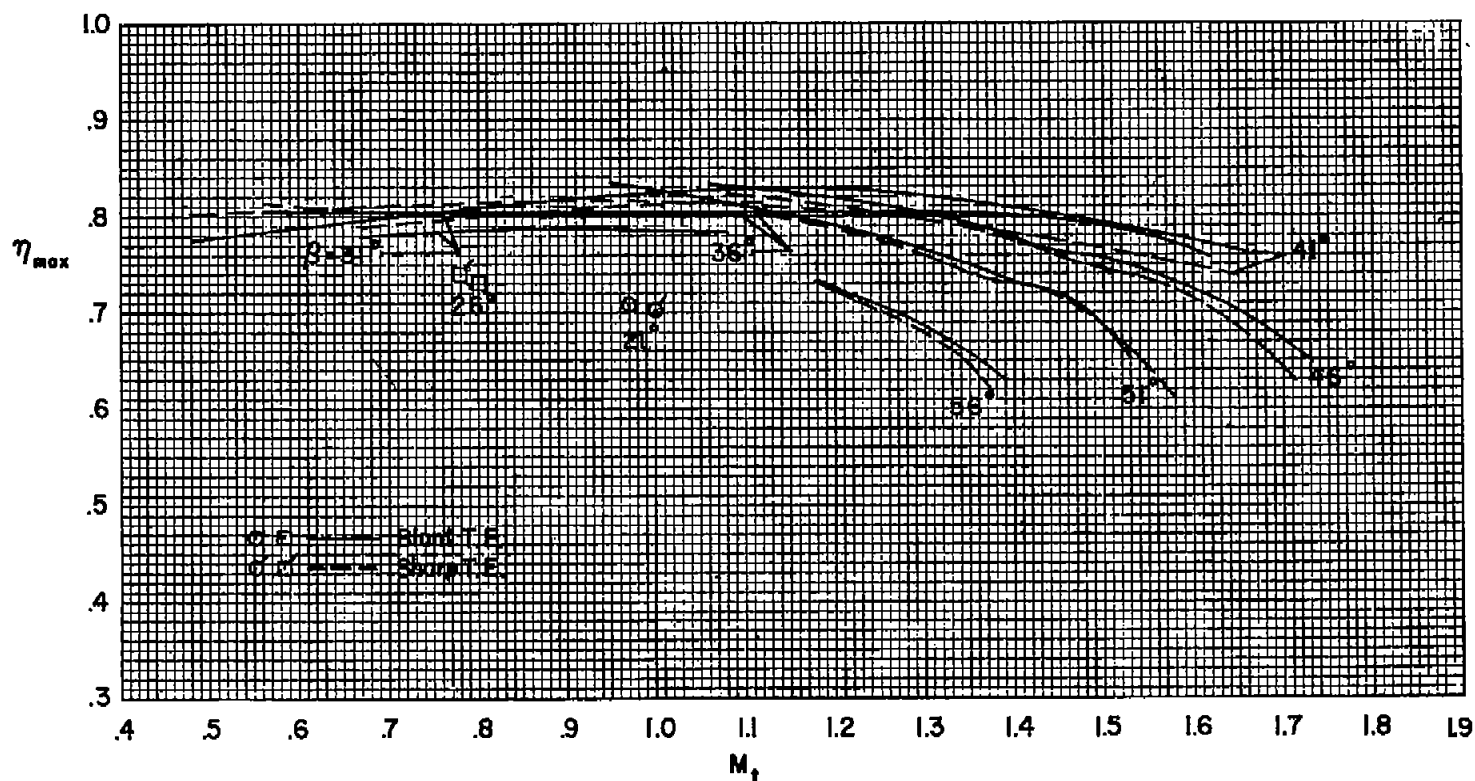


Figure 13.- The variation of maximum efficiency with tip Mach number for the blunt- and sharp-trailing-edge propellers; $R = 1,600,000$.

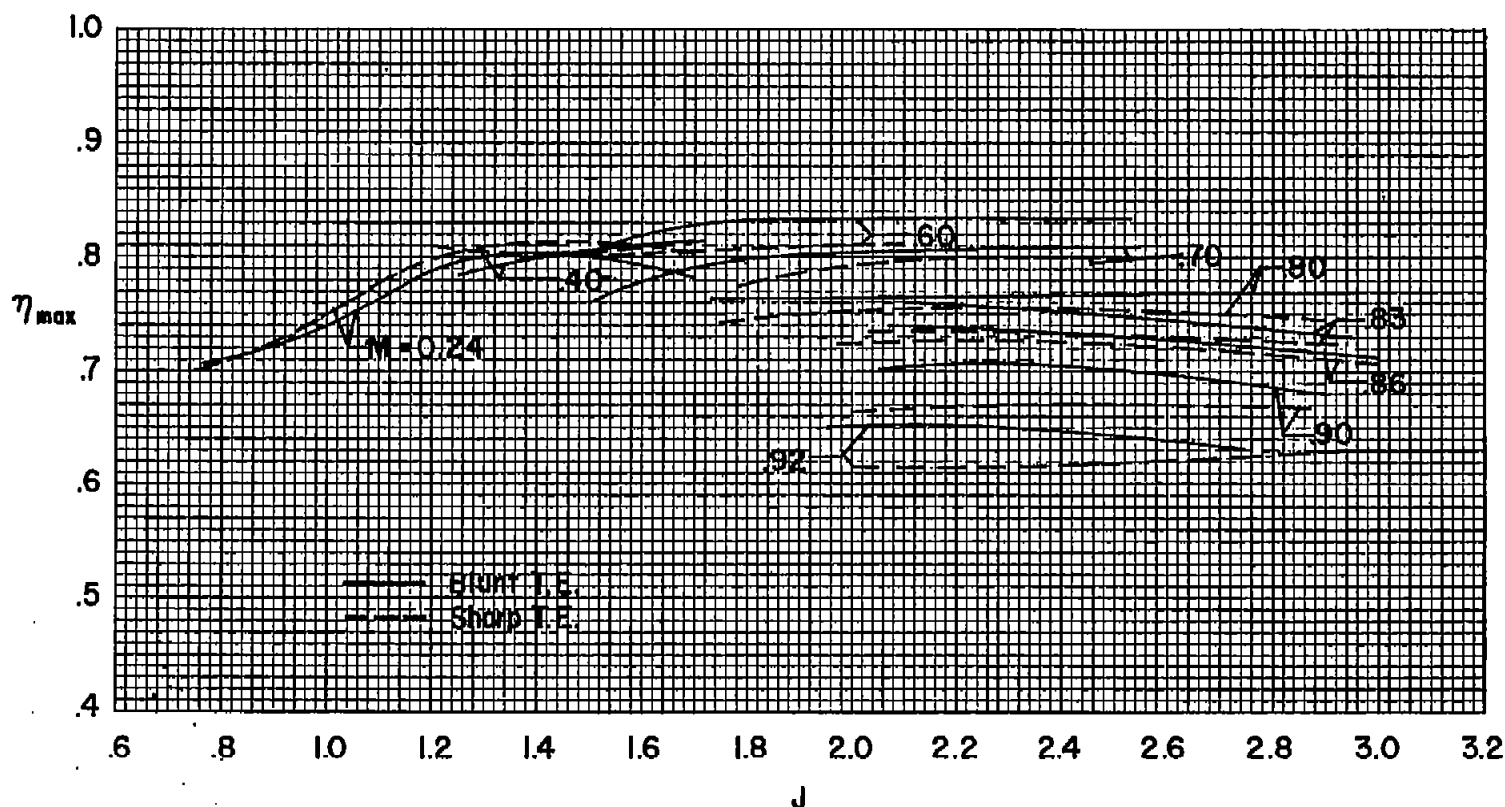
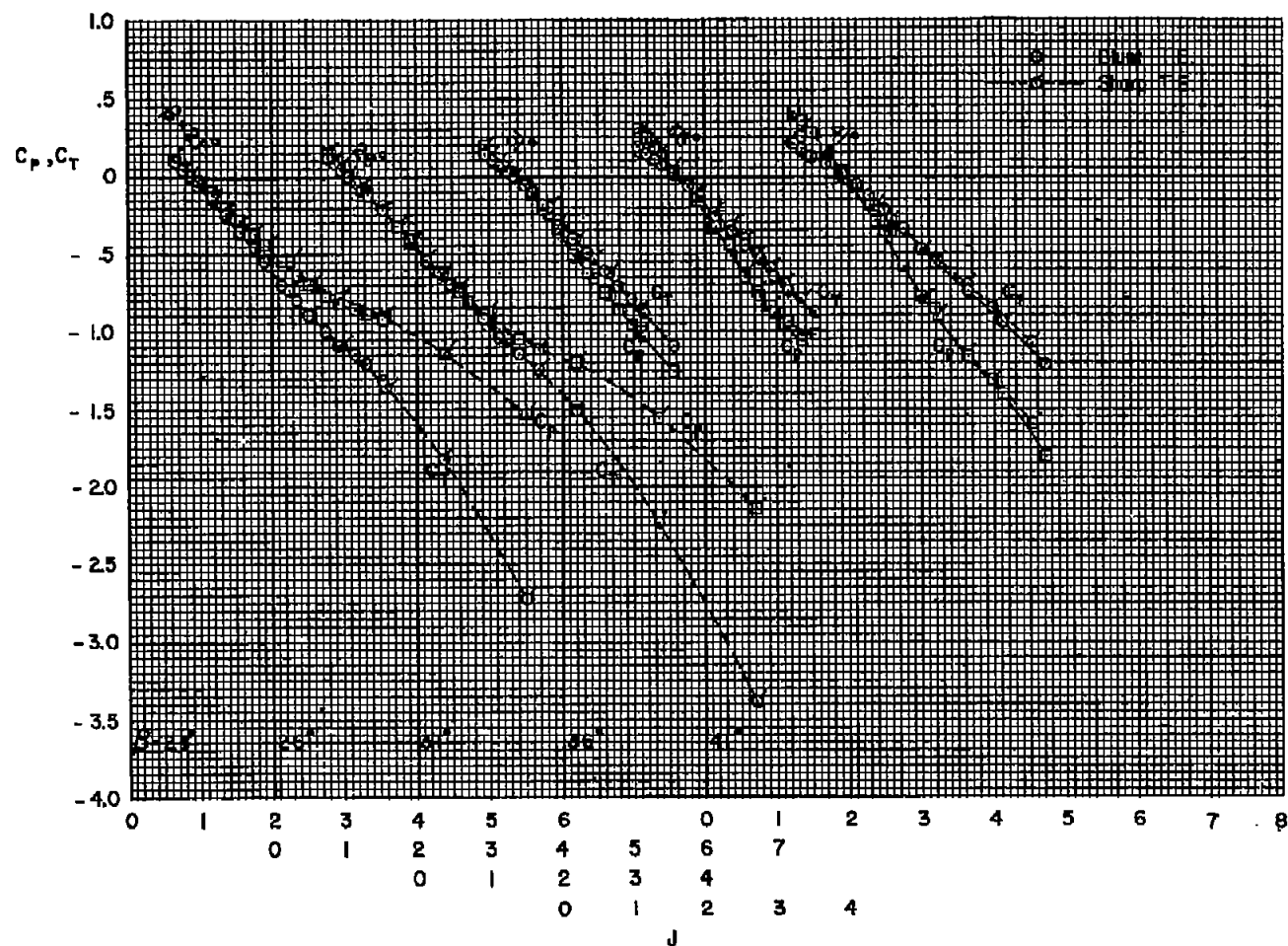
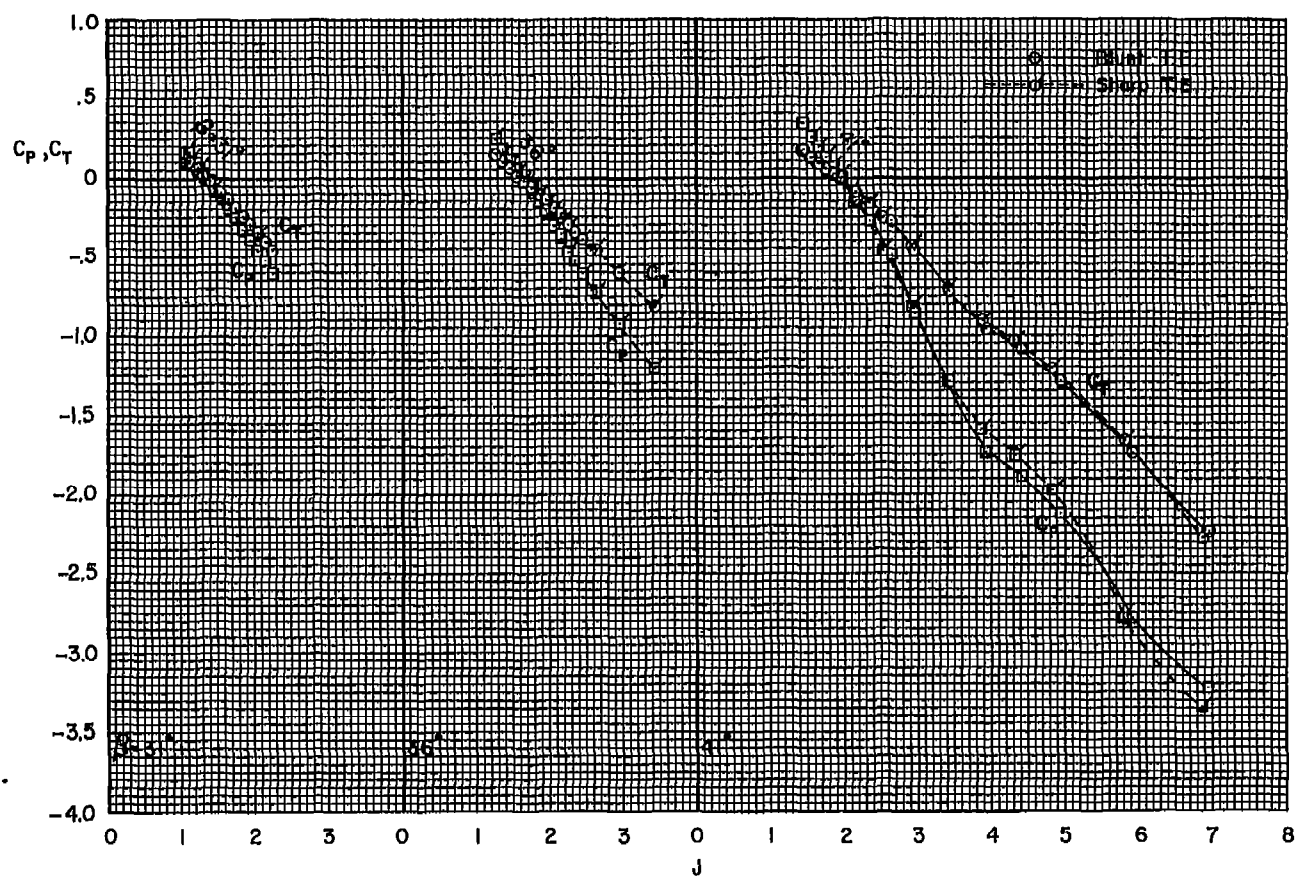


Figure 14.- The variation of maximum efficiency with advance ratio for the blunt- and sharp-trailing-edge propellers; $R = 1,600,000$.



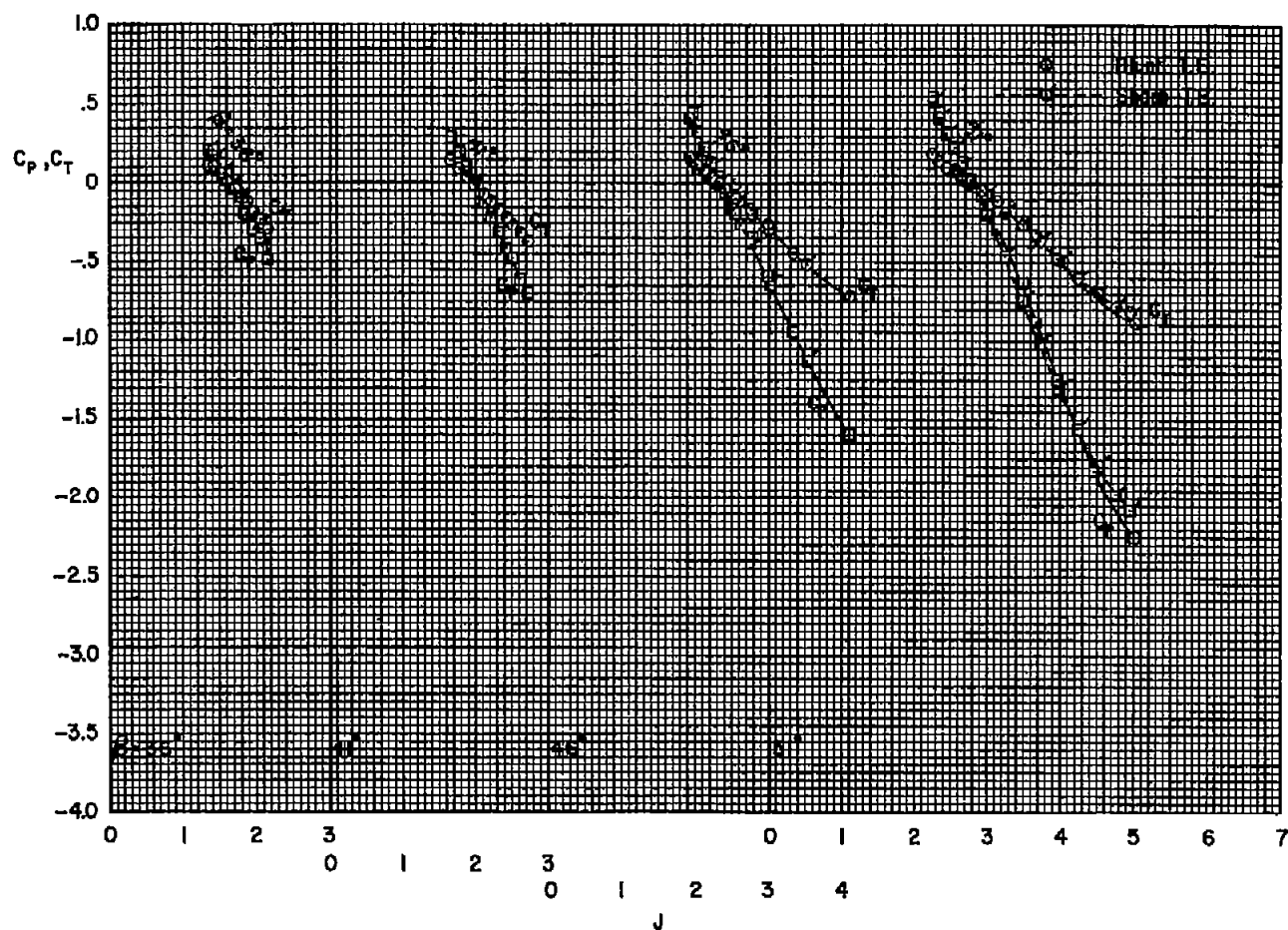
(a) $M = 0.24$

Figure 15.- The characteristics of the blunt- and sharp-trailing-edge propellers in primarily the negative-thrust range; $R = 1,600,000$.



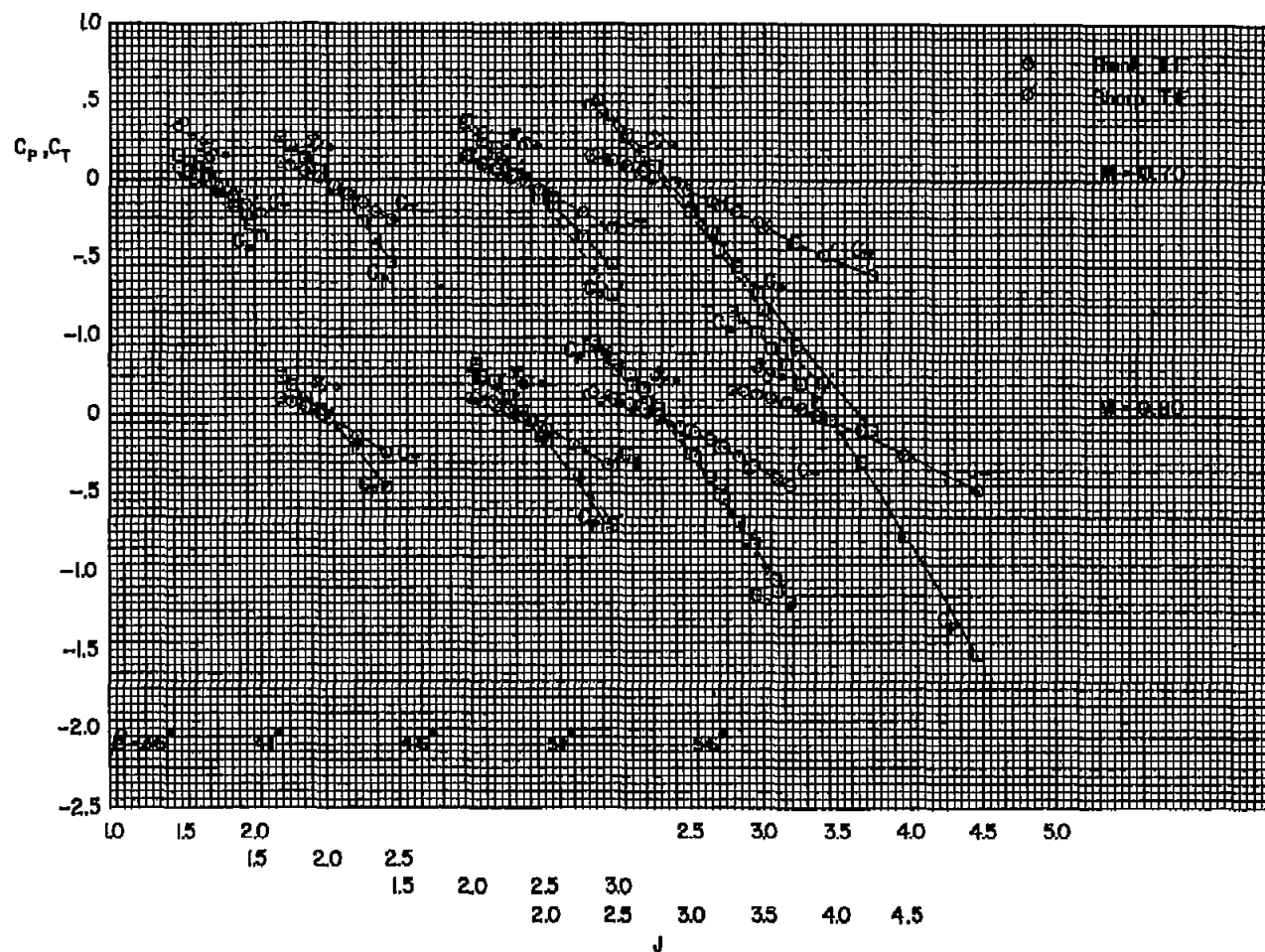
(b) $M = 0.40$

Figure 15.- Continued.



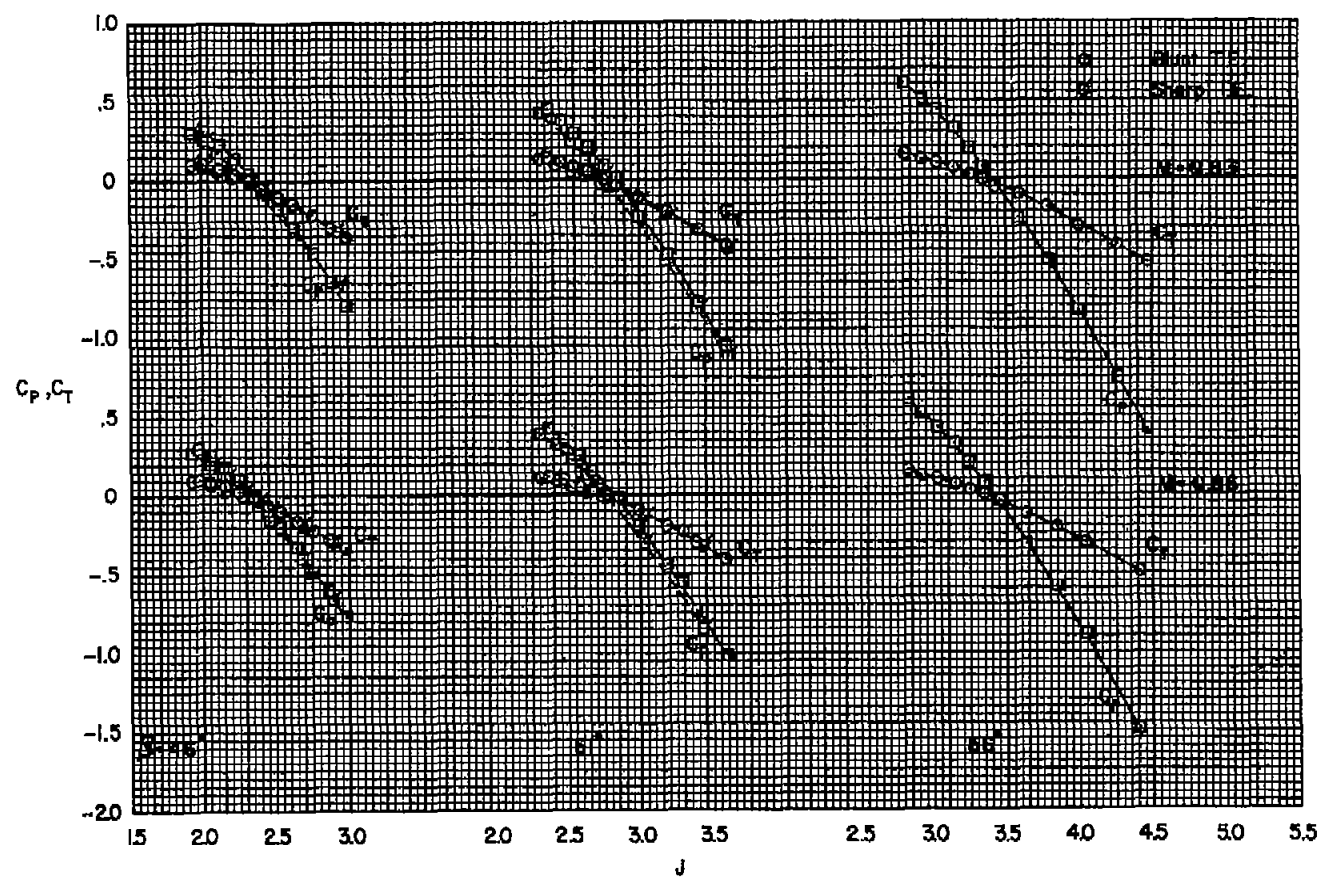
(c) $M = 0.60$

Figure 15.- Continued.



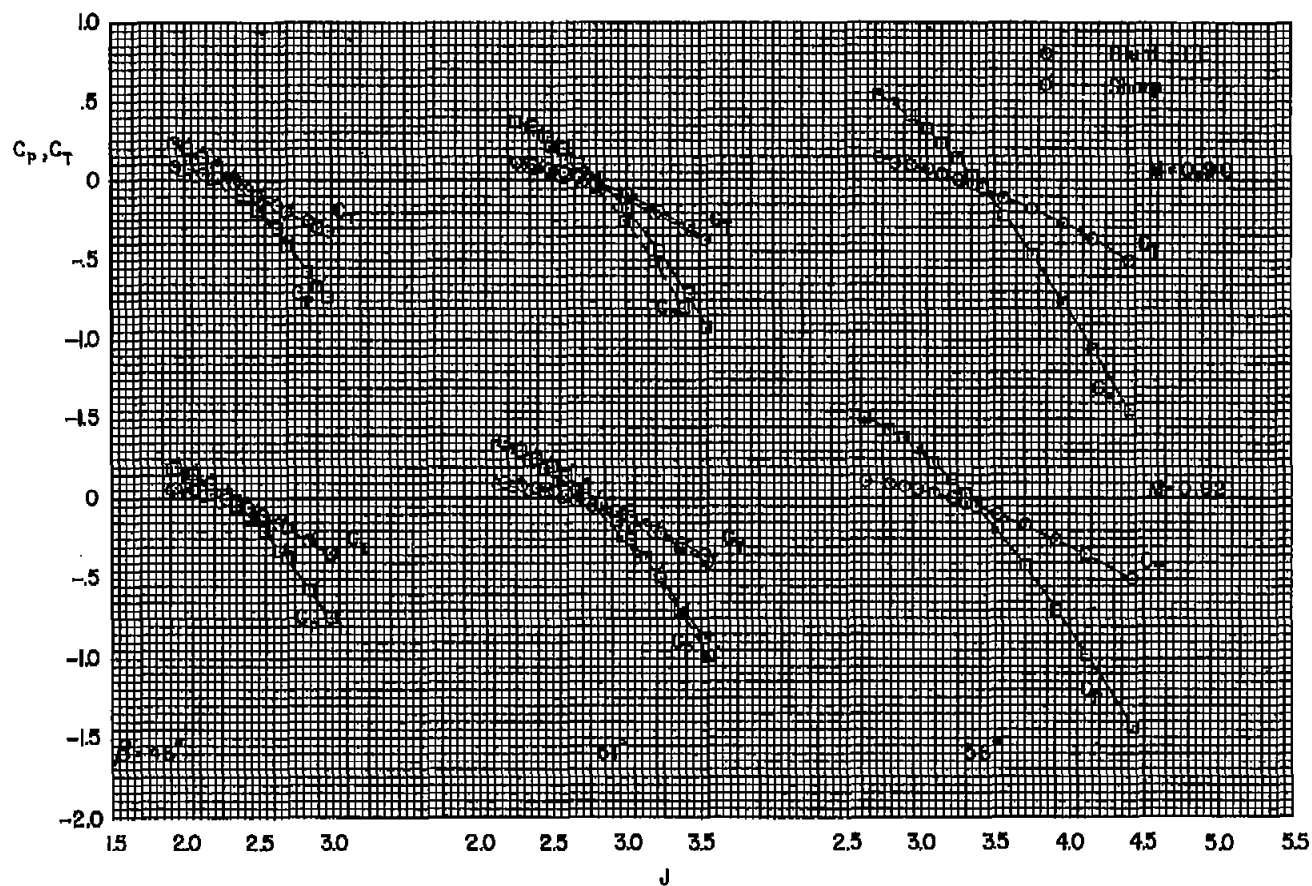
(d) $M = 0.70, 0.80$

Figure 15.- Continued.



(e) $M = 0.83, 0.86$

Figure 15.- Continued.



(f) $M = 0.90, 0.92$

Figure 15.- Concluded.

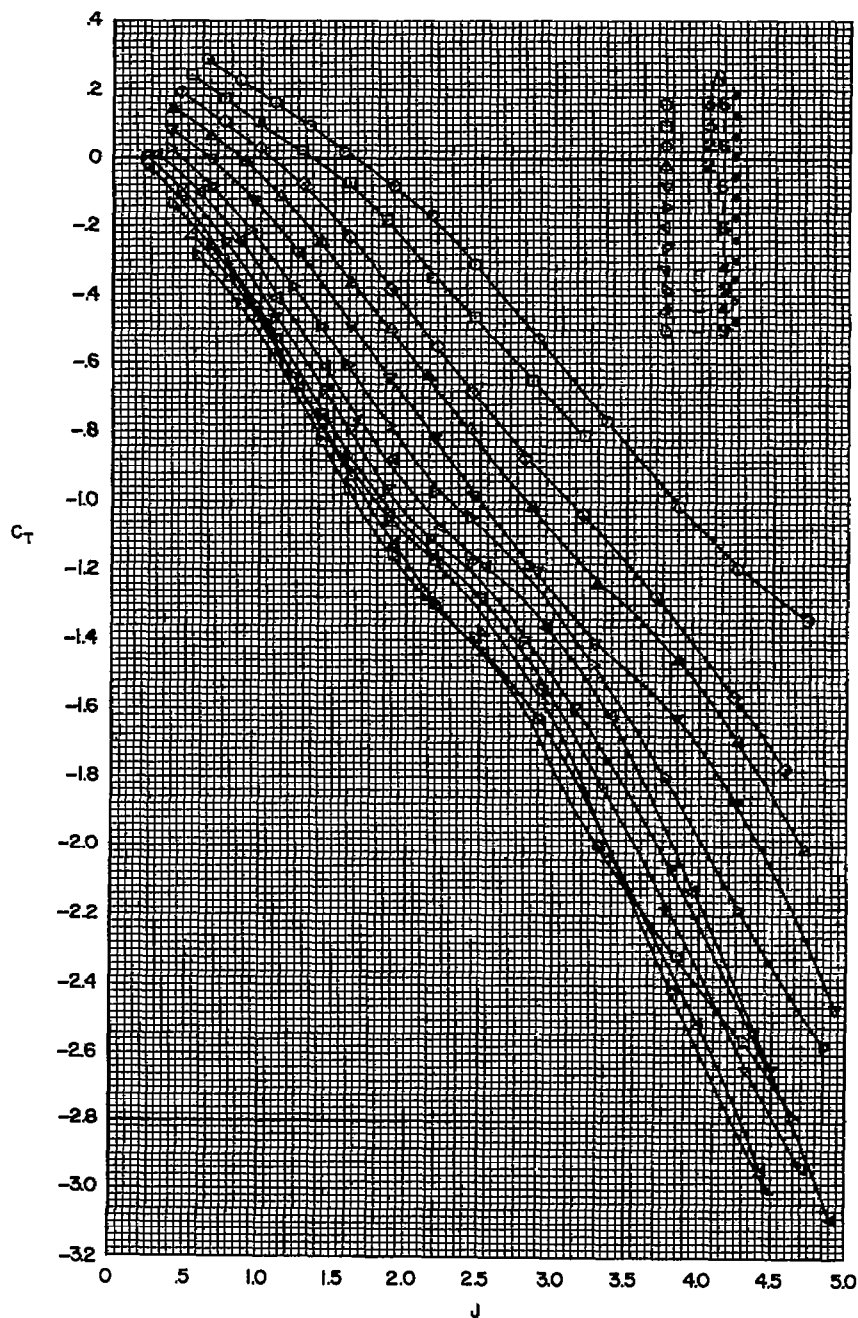
(a) C_T vs. J

Figure 16.- The characteristics of the blunt-trailing-edge propeller in primarily the negative-thrust range; $R = 1,150,000$, $M = 0.082$.

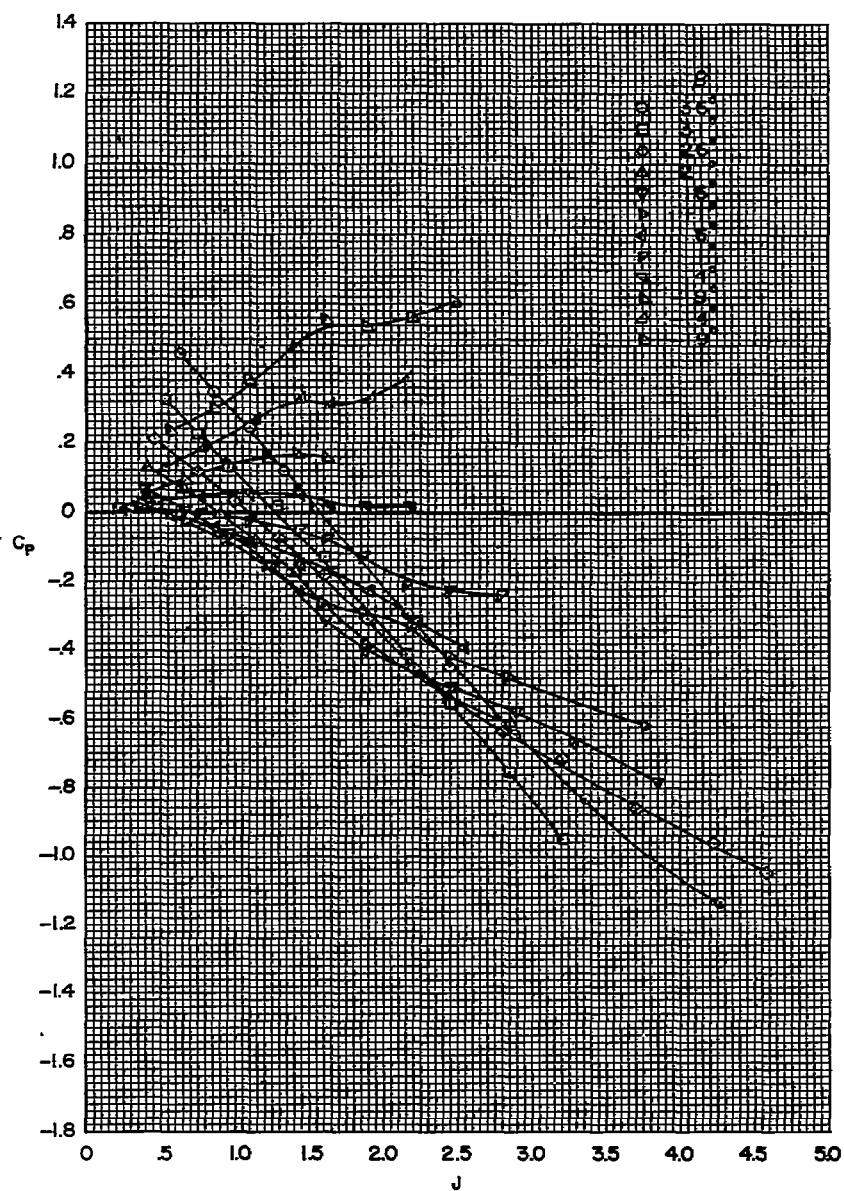
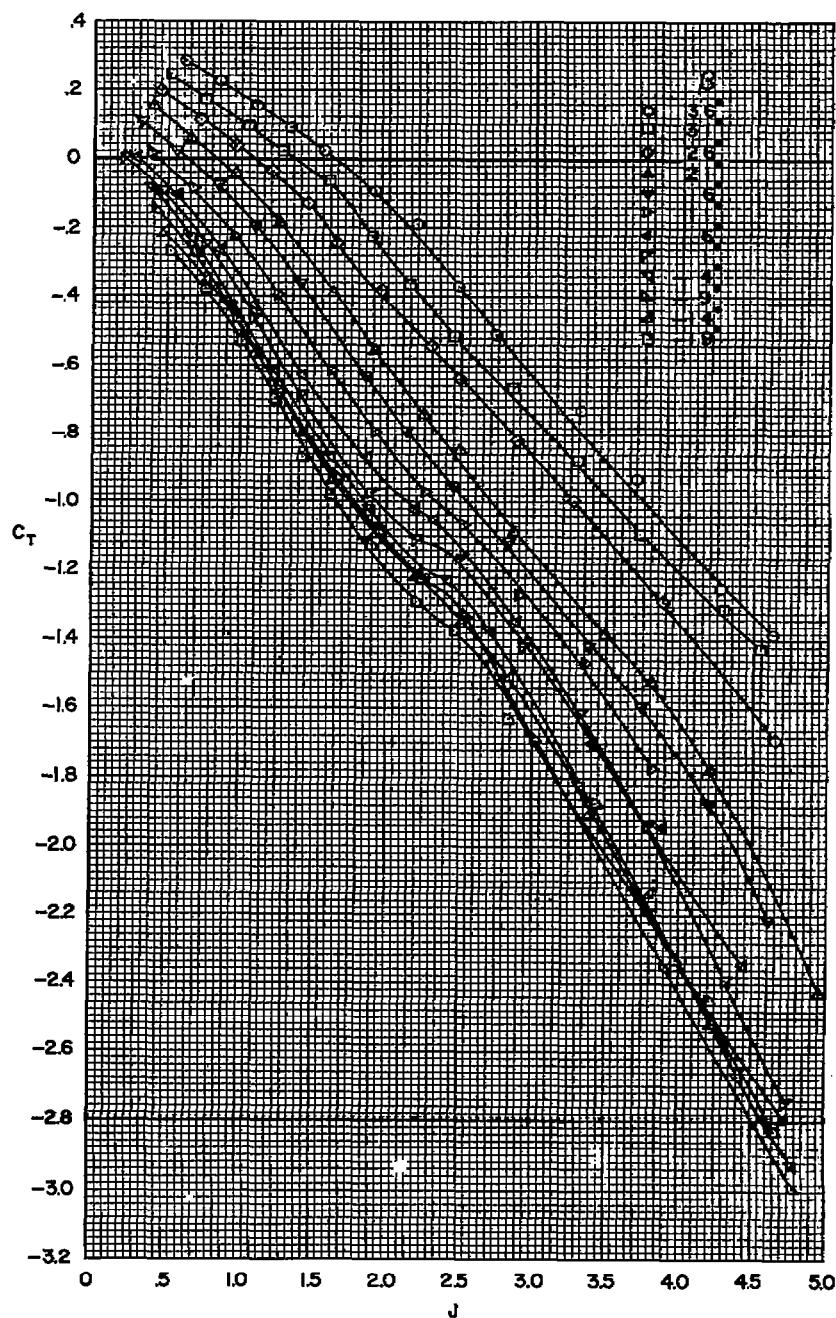
(b) C_p vs. J

Figure 16.- Concluded.



(a) C_T vs. J

Figure 17.- The characteristics of the sharp-trailing-edge propeller in primarily the negative-thrust range; $R = 1,150,000$, $M = 0.082$.

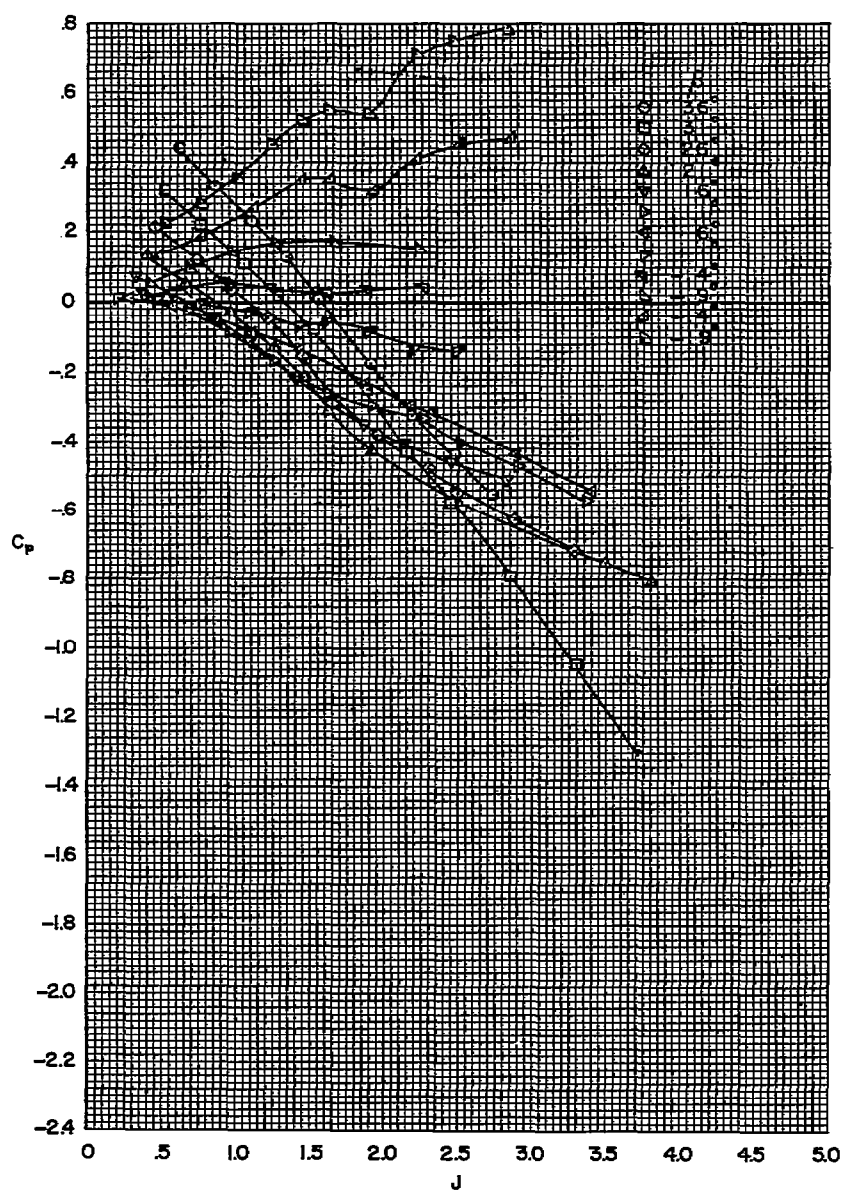
(b) C_p vs. J

Figure 17.- Concluded.

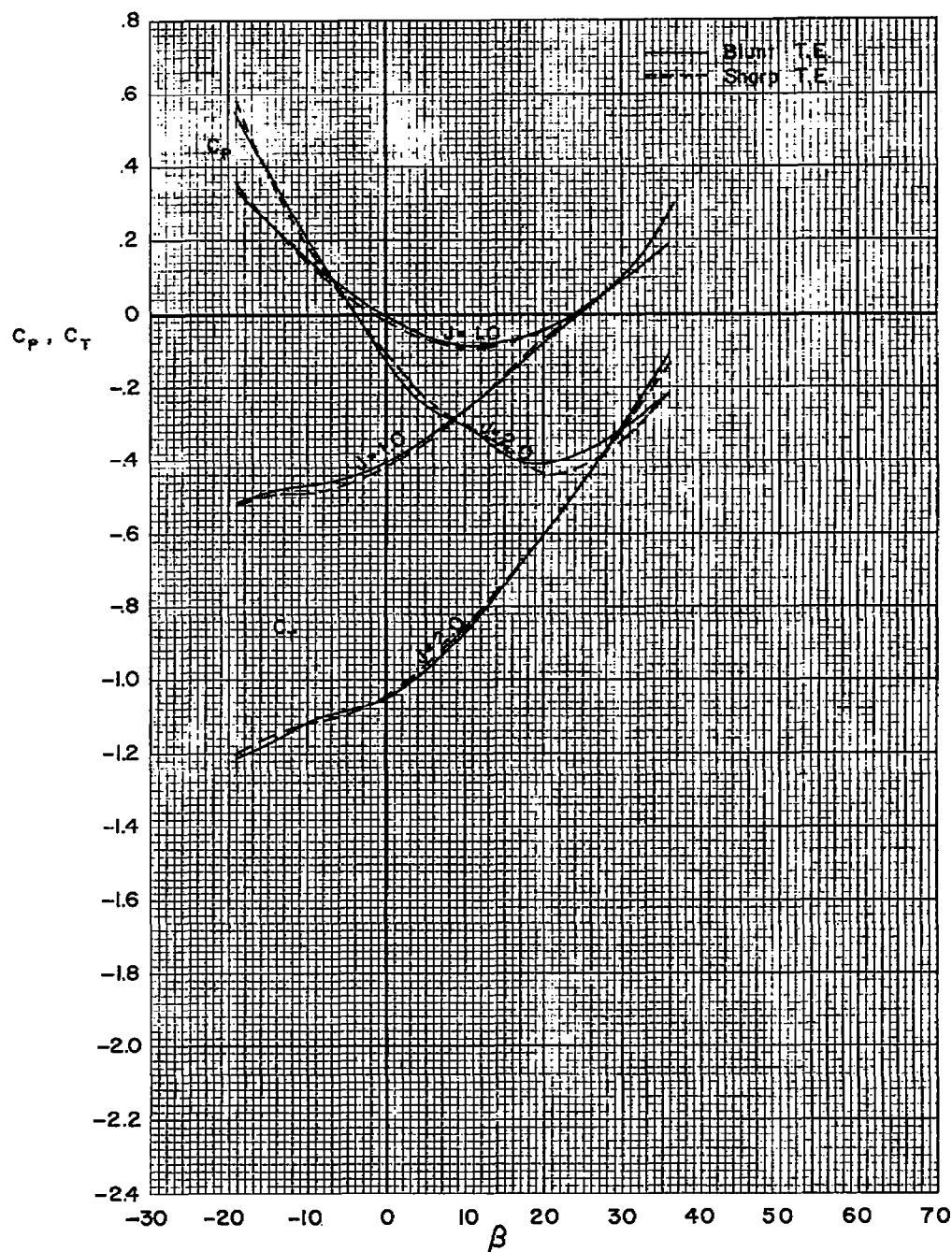


Figure 18.- The effect of blade angle on the characteristics of the blunt- and sharp-trailing-edge propellers in the negative-thrust range;
 $R = 1,150,000$, $M = 0.082$.

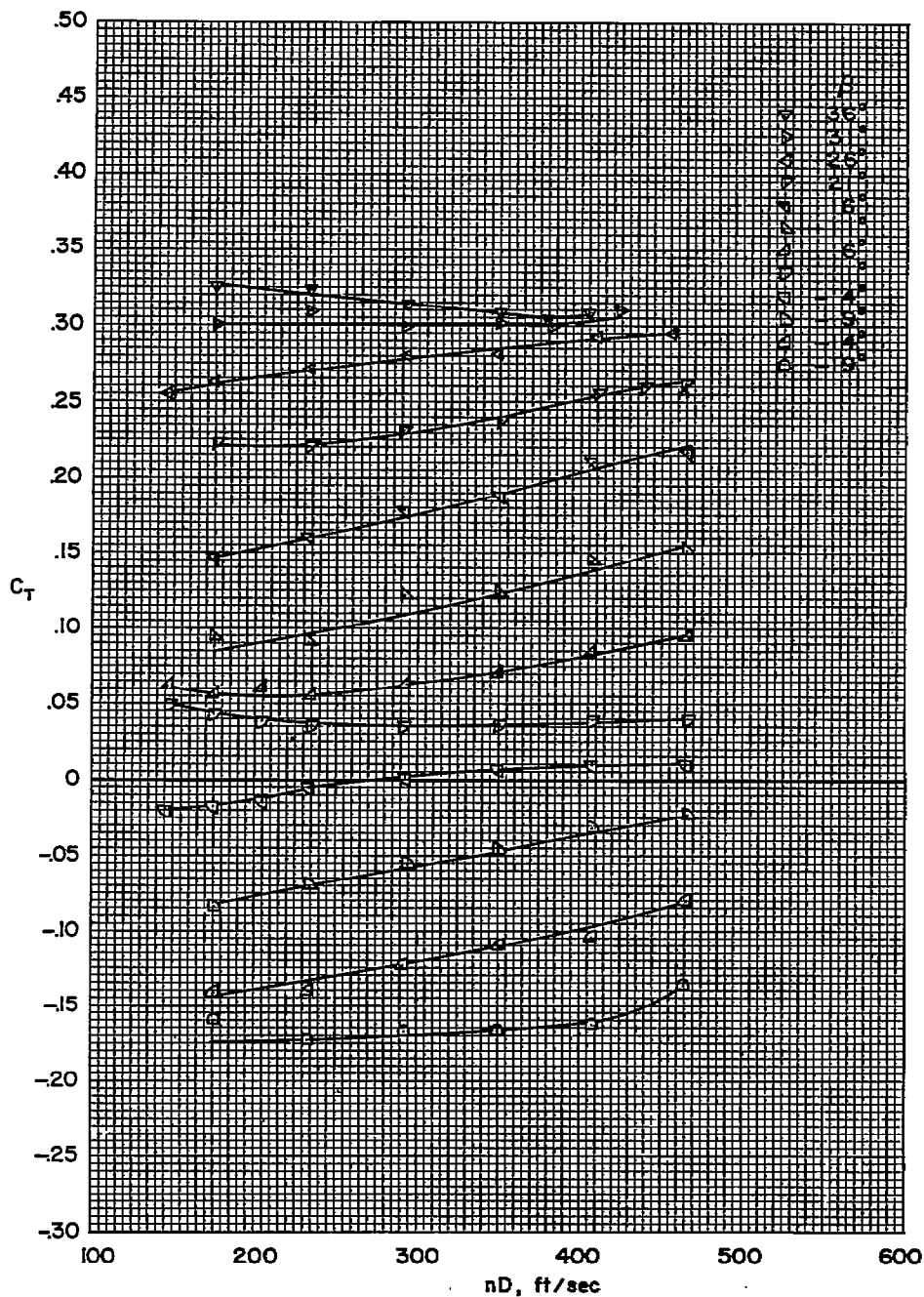
(a) C_T vs. nD

Figure 19.- Static characteristics of the blunt-trailing-edge propeller;
tunnel pressure = 3.3 lb/sq in. abs.

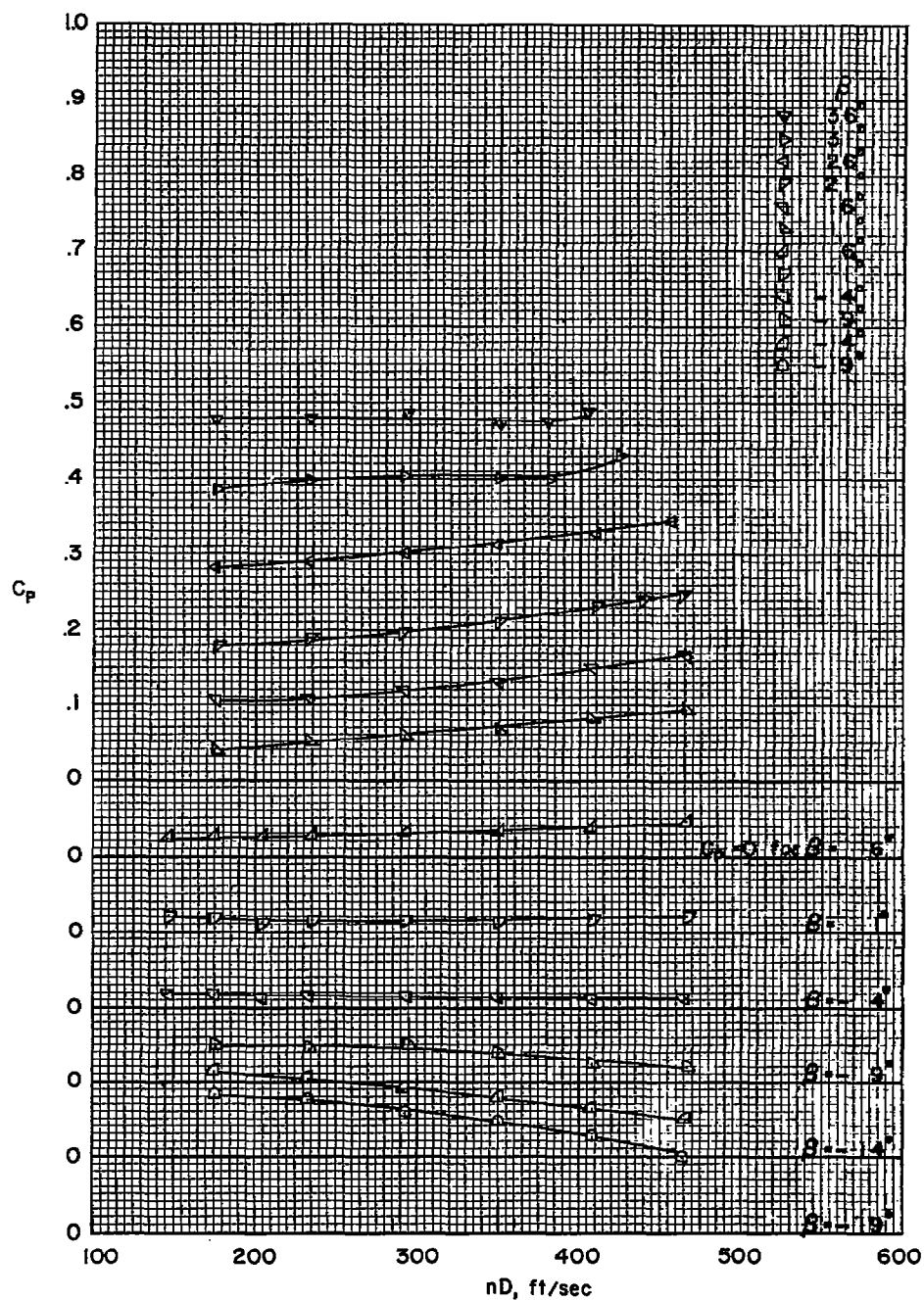
(b) C_p vs. nD

Figure 19.- Concluded.

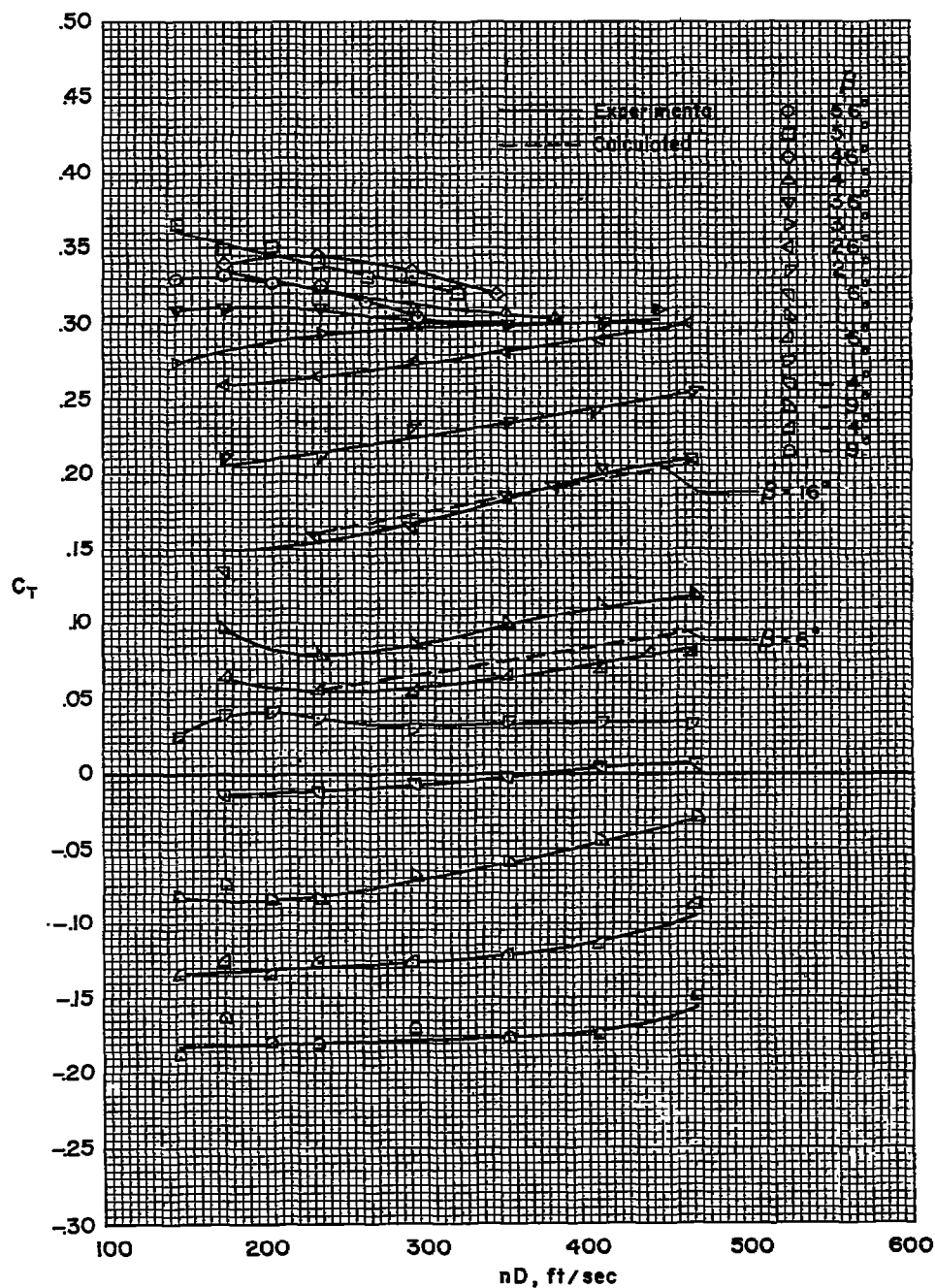
(a) C_T vs. nD

Figure 20.- Experimental and calculated static characteristics of the sharp-trailing-edge propeller; tunnel pressure = 3.3 lb/sq in. abs.

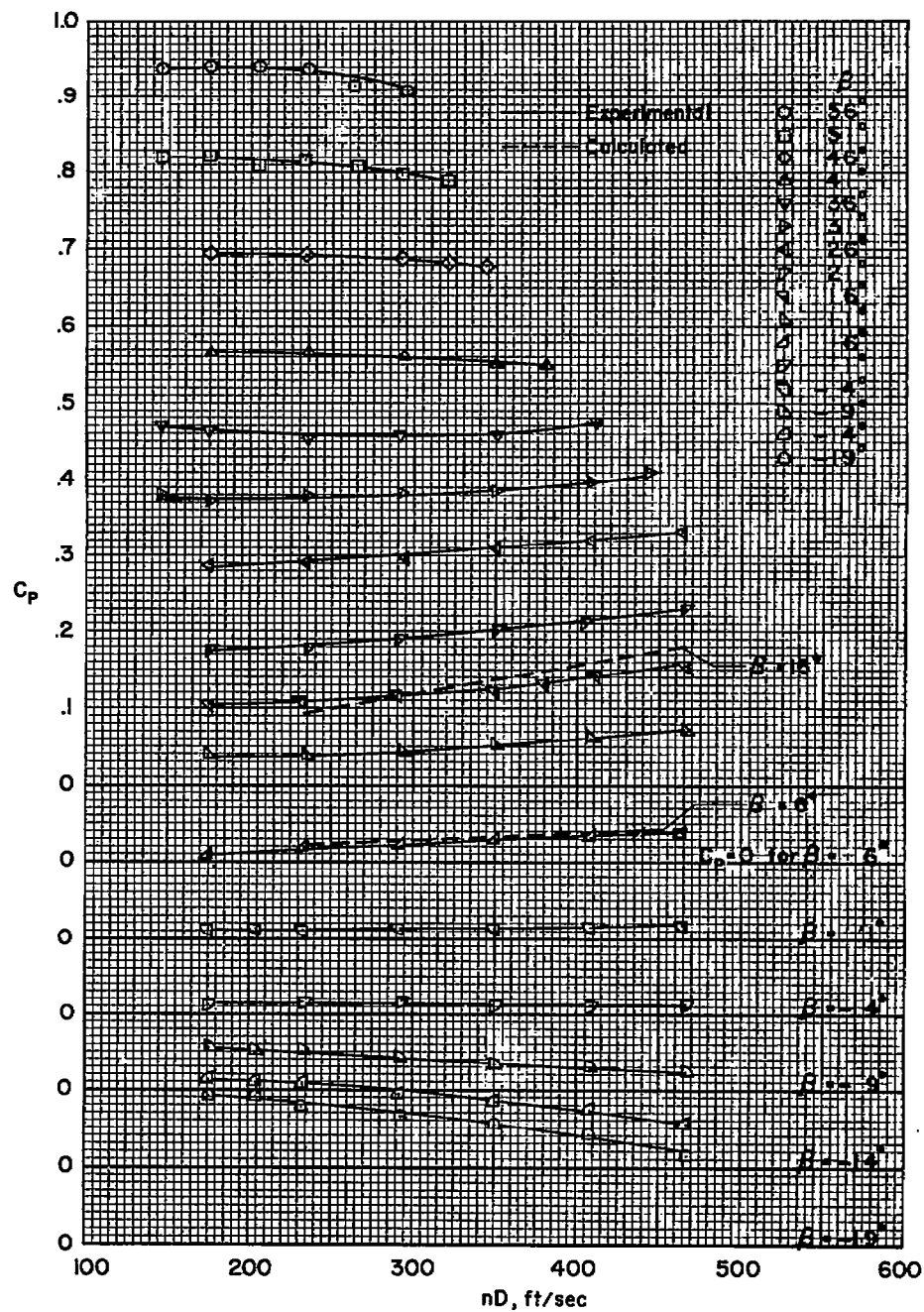
(b) C_p vs. nD

Figure 20.- Concluded.

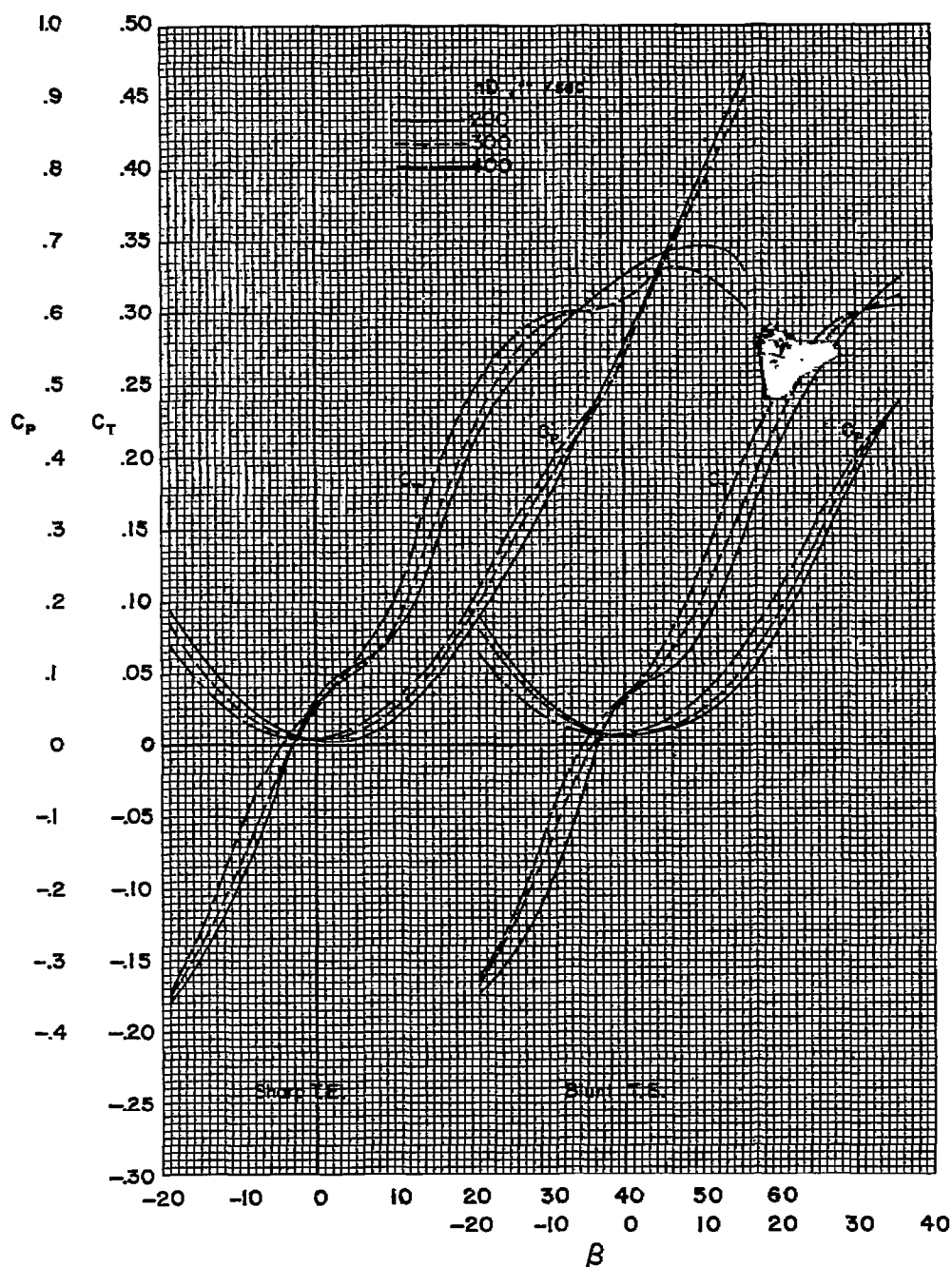
(a) C_T , C_p vs. β

Figure 21.- The variation with blade angle of the static characteristics of the blunt- and sharp-trailing-edge propellers; tunnel pressure = 3.3 lb/sq in. abs.

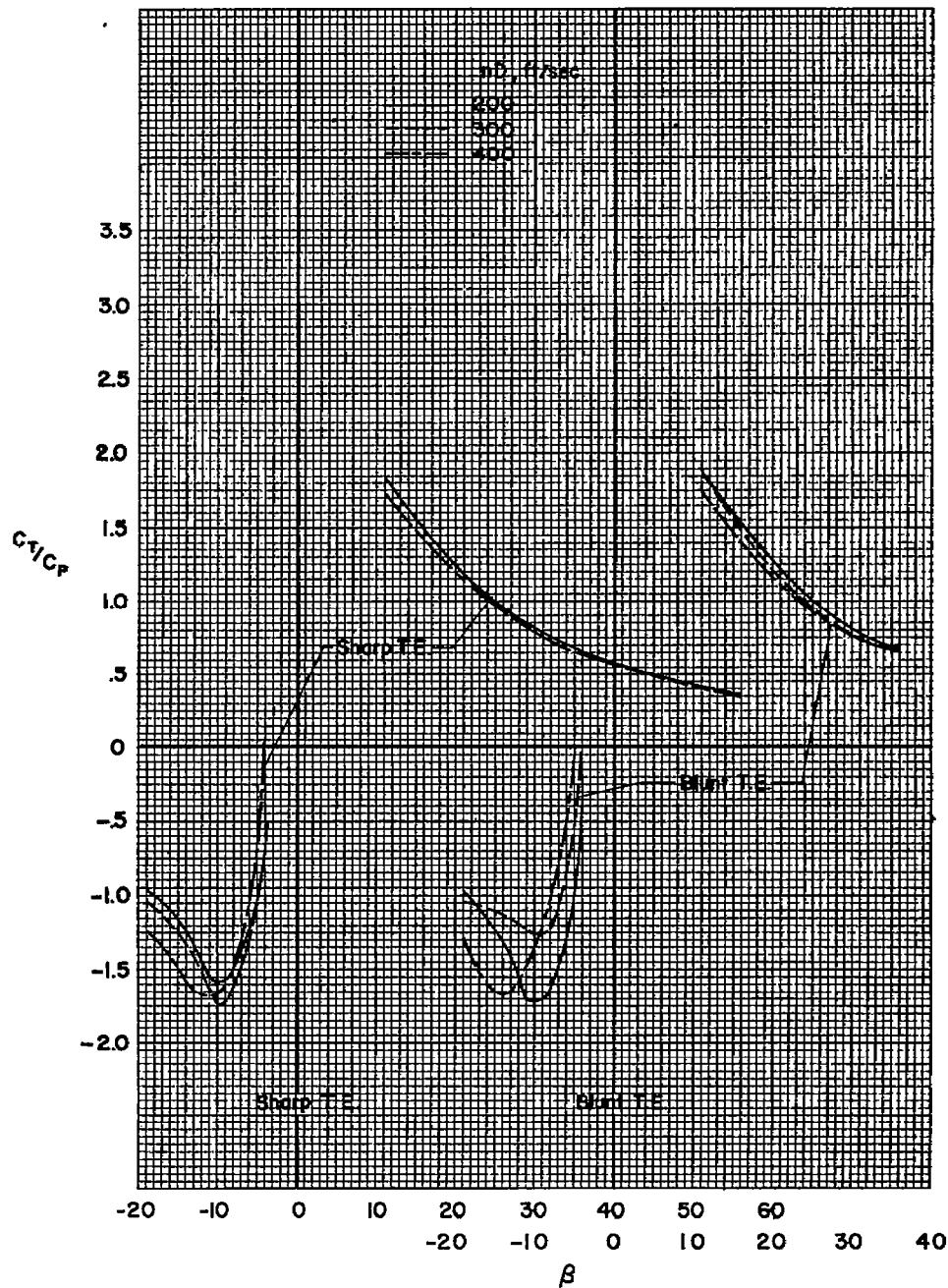
(b) C_T/C_P vs. β

Figure 21.- Concluded.

[REDACTED]



3 1176 01434 8545



1
1

1
1

1
1

[REDACTED]